

estimated by means of a fractionator-sampling design (Gundersen et al., 1988; West et al., 1991) and a former report (Baquet et al., 2005). Briefly, staining with the anti-TH antibody delineated the mediodorsal boundary of the SNC in each 60  $\mu\text{m}$  cryostat section. We used every third coronal section to perform an analysis starting with the first appearance of TH-positive neurons and extending to the most caudal parts of the SNC and including both hemispheres. Cell counts were made at automatically determined intervals by the StereoInvestigator, a morphometry and stereology software package (version 5.0; MicroBrightField, Colchester, VT), within an unbiased counting frame of known area ( $100 \times 100 \mu\text{m}^2$ ) superimposed on the image. Sections were viewed under  $40\times$  magnification on an Olympus (Tokyo, Japan) BA51 photomicroscope, the StereoInvestigator, thereby creating a systematic random sample of the area, randomly positioned the counting frame within the SNC. We defined 16  $\mu\text{m}$  as the z-dimension of the counting brick with a 2- $\mu\text{m}$  guard on each side. Stained cells were counted within the outlines defined by TH expression, and total estimates were obtained.

### Immunoblotting

After repeated rotenone administration for 28 days, the striatum (mixture of both right and left tissues) in treated mice were rapidly removed and homogenized with eight volumes of 50 mM Tris-buffered saline (pH 7.4) containing protease inhibitor cocktail (Roche Diagnostics, Mannheim, Germany). After centrifugation at 50,000g for 30 min, the supernatant was used as cytosolic fraction. Aliquots of cytosolic fractions containing 10  $\mu\text{g}$  of protein were subjected to sodium dodecyl sulfate-polyacrylamide gel electrophoresis (SDS-PAGE) and then immunoblotted with mouse monoclonal antibody against TH (1:5000) and reblotted with anti- $\beta$ -actin antibody (1:10,000). For semiquantitative analysis, bands of TH on radiographic films were scanned with a CCD color scanner (ARCUS II, AGFA, Leverkusen, Germany). Densitometric analysis was performed by the public domain program NIH Image 1.56 (by Wayne Rasband at the U.S. National Institutes of Health).

### Primary Neuronal Cultures of the Ventral Mesencephalon

Cultures of rat mesencephalic cells were established according to methods described previously (Sawada et al., 2004). Briefly, the ventral two-thirds of the mesencephalon were dissected from rat embryos on the 16th day of gestation. The dissected regions included dopaminergic neurons from the substantia nigra and the ventral tegmental area but not noradrenergic neurons from the locus ceruleus. Neurons were dissociated mechanically and plated out onto 0.1% polyethyleneimine-coated plastic coverslips at a density of  $1.3 \times 10^5$  cells/ $\text{cm}^2$ . The culture medium consisted of Eagle's minimum essential medium containing 10% fetal calf serum for the first 1–4 days in culture and horse serum from the 5th day onward. Cultures were maintained at 37°C in a humidified atmosphere of 5%  $\text{CO}_2$ . Only mature cultures (8 days in vitro) were used for experiments. The animals were treated in

accordance with guidelines published in the NIH Guide for the Care and Use of Laboratory Animals.

### Treatment of Cultures

All experiments were carried out in Eagle's minimum essential medium with 10% horse serum at 37°C. First of all, cultured neurons were exposed to rotenone for 48 hr, except for pretreatment of LY294002 for 10 min to cause PI3K inhibition. After that, to show the time course, cultured neurons were administered rotenone and/or nicotine for 12, 24, and 48 hr. Nicotine and nAChR antagonists (Mec,  $\alpha\text{BuTx}$ , DH $\beta\text{E}$ ) were added to the medium simultaneously with rotenone. The concentration of each antagonist was the maximal dosage that did not show cytotoxicity or interference among nAChRs. Ki values of  $\alpha\text{BuTx}$  were 2.16 (1.56–3.01) nM for  $\alpha 7$  nAChR and  $>10,000$  nM for  $\alpha 4\beta 2$  nAChR, and those of DH $\beta\text{E}$  were 7700 (4510–13,100) nM for  $\alpha 7$  nAChR and 24.6 (16.9–35.8) nM for  $\alpha 4\beta 2$  nAChR (Grinevich et al., 2005). To confirm PI3K inhibition, LY294002 was administered 10 min before the additional treatment of rotenone and nicotine. Triciribine was used simultaneously with rotenone and nicotine to inhibit Akt/PKB.

### Immunocytochemistry and Evaluation of Neurotoxicity in Neuronal Cultures

Immunostaining was used to evaluate the number of dopaminergic neurons. Cultured cells were incubated with polyclonal rabbit anti-TH antibody (1:400) overnight at 4°C, then with biotinylated secondary antibody (1:200), and conjugated to avidin peroxidase (1:200) by the ABC kit (Vector Laboratories, Burlingame, CA) at room temperature for 1 hr. After that, they were labeled with a DAB staining kit (Nacalai, Kyoto, Japan). Neurotoxicity in each experiment was defined as a reduction in the survival rate, which was expressed as percentage survival relative to the survival observed in control cultures. For primary cultures, at least 200 dopaminergic neurons were counted in 30 randomly selected fields at  $100\times$  (total magnification) in control cultures to determine the total number of neurons. The total number of neurons was assessed by the method, described above, but using the anti-MAP2 antibody.

### RNA Preparation From Rat Mesencephalic Cells

Total cell RNA was extracted with the Isogen RNA Isolation Kit (Nippon Gene, Japan) as originally described elsewhere (Chomczynski and Sacchi, 1987). The concentration of the isolated total RNA was determined spectrophotometrically at 260 nm. The first strand cDNA was synthesized with a reverse transcriptase-polymerase chain reaction (RT-PCR) kit purchased from GE Healthcare Bioscience (Giles, UK). Briefly, reverse transcription (RT) was carried out in a 15- $\mu\text{L}$  reaction mixture containing 5  $\mu\text{g}$  total RNA, 5  $\mu\text{L}$  Bulk first-strand reaction mix, 1  $\mu\text{L}$  DTT solution, and 1  $\mu\text{L}$  pd(N)<sub>6</sub> primer, by incubation at 42°C for 20 min followed by denaturation at 99°C for 5 min and then quick-chilled on ice. The second strand cDNA synthesis/PCR amplification was performed in a mixture of 2  $\mu\text{L}$  RT product, 2.5  $\mu\text{L}$   $10\times$  PCR buffer, 200 nM dNTP, 1.5 mM  $\text{MgCl}_2$ , 0.05 U/ $\mu\text{L}$  Ex

**TABLE I. Paired Primers Used for RT-PCR Detection of nAChR Subunits\***

Subunit	Primer	Nucleotide sequence	Size (bp)	T <sub>m</sub> (°C)
α4	Forward	CTGGGTGCGTAGAGTCTTCC	239	62
	Reverse	TAGGCTGGGTCTCGACTGCT		
α7	Forward	TTTCTGCGCATGAAGAGGCCCGGAGAT	295	60
	Reverse	ACCTCCTCCAGGATCTT		
β2	Forward	AAGGTGGTCTTCCCTGGAGAAGC	287	60
	Reverse	GCGTACGCCATCCACTGCT		
GAPDH	Forward	CGTCTTACCACCATGGAGA	300	60
	Reverse	CGGCCATCACGCCACAGCTT		

\*T<sub>m</sub>, annealing temperature; Forward, sense primer; Reverse, antisense primer. GAPDH (glyceraldehyde-3-phosphate dehydrogenase) was used as the internal control for RNA detection.

Taq DNA polymerase, and 500 nM sense and antisense primers (Table I). The amplification protocol was as follows: initial denaturation at 94°C for 5 min; 30 cycles at 94°C for 30 sec, annealing at the respective temperature (Table I) for 30 sec, and 72°C for 1.5 min; a final extension at 72°C for 7 min with a GeneAmp 9700 thermal cycler (Perkin Elmer, Applied Biosystem, Foster City, CA). PCR products were electrophoresed on 2% agarose gels and stained with ethidium bromide (0.5 mg/mL). Then, the PCR products were visualized with an ultraviolet transilluminator coupled to a CCD camera.

#### Statistical Evaluation

Data was expressed as the ratio of surviving dopaminergic neurons relative to the number of neurons in vehicle-treated or in control group. Also, the density of TH by immunoblotting was assessed in the same manner. They are represented as the mean ± SEM. Statistical significance was determined by analysis of variance (ANOVA) followed by Bonferroni's multiple comparison test.

## RESULTS

### Nicotine Treatment Improved Behavior Impaired by Rotenone

In our *in vivo* studies, we first checked the motor behavior of rotenone-treated model mice because it was important that the animals showed a close PD phenotype. The simultaneous daily administration of oral rotenone and subcutaneous nicotine prevented the motor impairment elicited by rotenone (Fig. 1). Nicotine alone showed no significant difference compared with the vehicle group. This animal model could be useful for assessing the bradykinesia/akinesia, one of the symptoms of PD.

### Nicotine Treatment Improved Histological Findings in the Substantia Nigra

In the substantia nigra, oral treatment of rotenone decreased the number of dopaminergic neurons. On the other hand, the simultaneous daily administration of oral rotenone and subcutaneous nicotine prevented the decrease (Fig. 2A). Stereological assessment of the number of TH-positive cells in the bilateral SNC confirmed the histological findings with the statistical significance

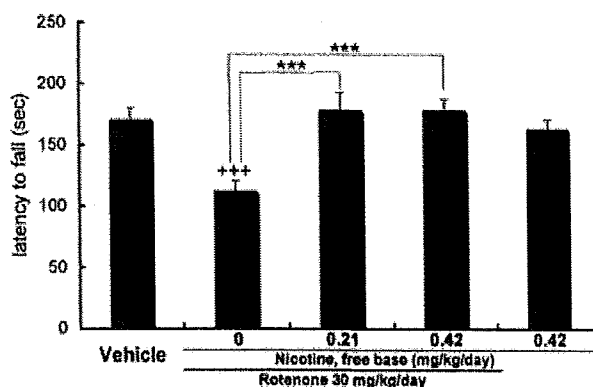


Fig. 1. Behavior analysis by rotarod treadmill test of chronically rotenone-treated mice. Nicotine administration improved impaired behavior induced by rotenone. One-way ANOVA was used for statistical analysis, followed by Bonferroni's multiple comparison test. Each value is the mean ± SEM,  $n = 8-12$ , \*\*\* $p < 0.001$ , +++ $p < 0.001$  vs. vehicle.

(Fig. 2B). That is, simultaneous administration of nicotine significantly protected dopaminergic cells in the midbrain of rotenone-treated mice from rotenone-induced neurotoxicity.

### Nicotine Attenuated Rotenone-induced Axonal/Nerve Terminal Damage in the Striatum

The striatum was immunostained with the same antibody as the substantia nigra. About histological findings, the density of TH-positive neurons in the striatum of rotenone-treated mice seemed to be diminished compared with the vehicle group. Rotenone and nicotine treatment seemed to prevent the density from being decreased (Fig. 3A). Densitometric analysis of immunoblotting performed using the striatal lysate of each group showed that nicotine treatment remarkably improved the expression of TH from rotenone toxicity (Fig. 3B). In other words, these results confirmed that nicotine protected nigrostriatal dopaminergic neurons from the cell death by rotenone toxicity. α-Synuclein-positive aggregations were detected in the cell bodies of dopaminergic neurons of rotenone-treated mice, but the number was

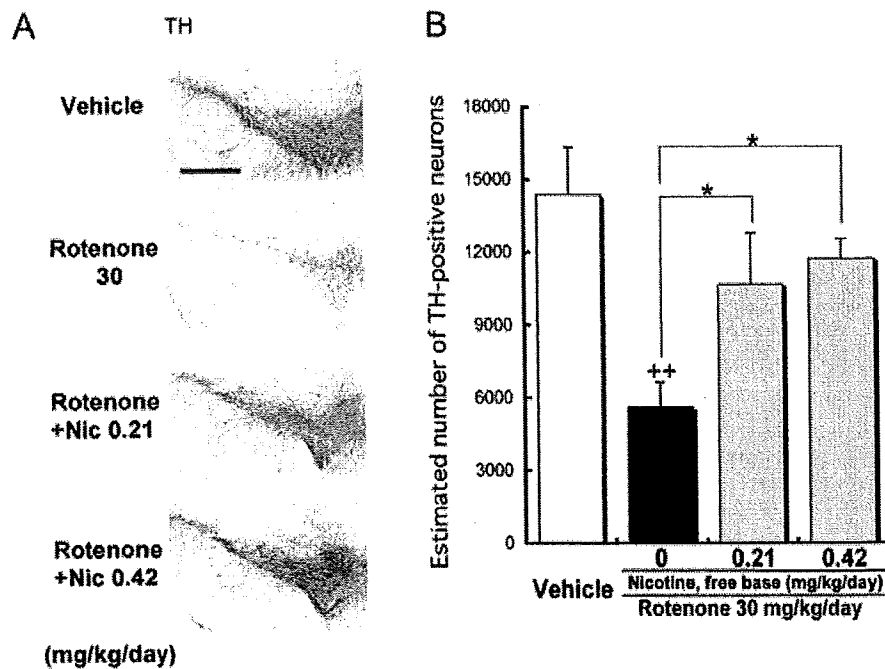


Fig. 2. Immunohistological analysis of nigral dopamine neurons. Nicotine improved the viability of dopaminergic cells against rotenone toxicity. Nic, Nicotine. **A:** Representative findings of each group. Scale bar = 500  $\mu$ m. **B:** Stereological analysis of the number of the TH-positive neurons in the substantia nigra. One-way ANOVA was used for statistical analysis, followed by Bonferroni's multiple comparison test. Each value is the mean  $\pm$  SEM,  $n = 4$ , \* $P < 0.05$ , ++ $P < 0.01$  vs. vehicle.

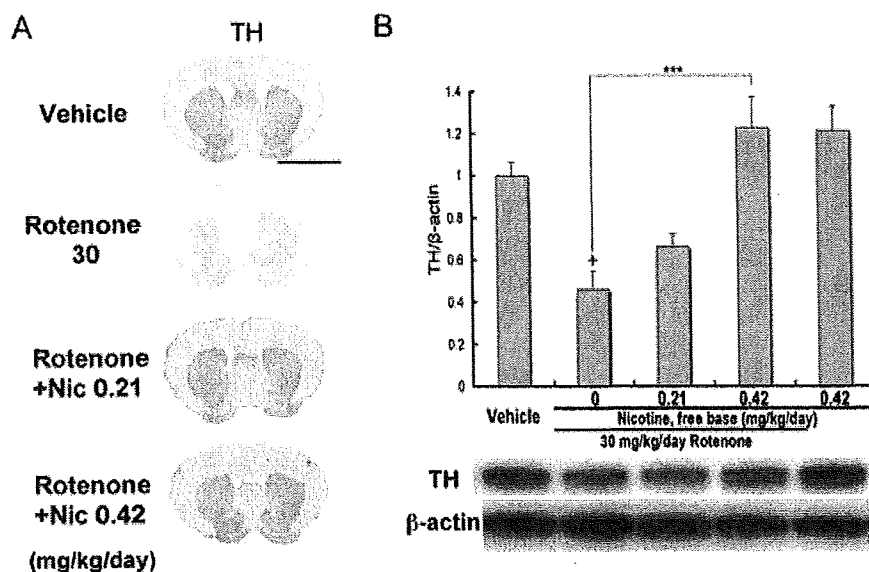


Fig. 3. Immunological analysis of striatal dopamine neurons. Nicotine improved the viability of dopaminergic cells against rotenone toxicity. **A:** Representative immunohistological findings of each group. Nic, Nicotine. Scale bar = 4 mm. **B:** Densitometric analysis of TH in striatal lysate. TH density was expressed as TH/β-actin ratio and relative density standardized by the results of vehicle group. One-way ANOVA was used for statistical analysis, followed by Bonferroni's multiple comparison test. Each value is the mean  $\pm$  SEM,  $n = 4$ , \*\*\* $P < 0.001$ , + $P < 0.05$  vs. vehicle.

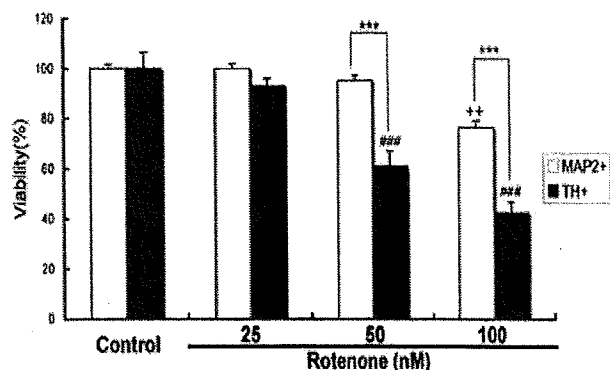


Fig. 4. Statistical analysis of rotenone-induced neuronal cell death in cultures of rat mesencephalic cells (day 8), standardized by the number of sham operations. It was suggested that dopaminergic neuron was more vulnerable against rotenone toxicity than other types of neurons. MAP2, microtubule-associated protein 2, a marker of central nervous system neurons; TH, tyrosine hydroxylase, a marker of dopaminergic neurons. Two-way factorial ANOVA was used for statistical analysis, followed by Bonferroni's multiple comparison test. Each value is the mean  $\pm$  SEM,  $n = 8$ ,  $***P < 0.001$ ,  $^{++}P < 0.01$  vs. control (MAP2 positive),  $###P < 0.001$  vs. control (TH positive).

too small to perform statistical assessment (data not shown).

#### Neuroprotective Effect of Nicotine Against Rotenone-induced Neurotoxicity in Cultures of Mesencephalic Neurons

Forty-eight-hour exposure to rotenone caused dose-dependent neurotoxicity, more remarkable in TH-positive neurons than in MAP2-positive cells, which represented the total neuronal cells (Fig. 4). This result showed that dopaminergic neurons were more vulnerable to rotenone-induced neurotoxicity. Time course experiment revealed that both rotenone toxicity and nicotinic neuroprotection were shown remarkably after 24 hr (Fig. 5). Immunostaining of TH showed that the viability of TH-positive cells was decreased by rotenone treatment and improved by addition of nicotine. Treatment with nicotine alone did not remarkably change the viability of TH-positive cells statistically (Fig. 5, Fig. 6A–D). Simultaneous administration of nicotine resulted in a dose-dependent increase of the viability of TH-positive cells (Fig. 6E). So nicotine treatment protected dopaminergic neurons against rotenone-induced neuronal death in a dose-dependent manner. This neuroprotective effect was inhibited by 100  $\mu$ M Mec, a broad-spectrum nAChR antagonist (Fig. 7A), 100 nM  $\alpha$ BuTx, an  $\alpha$ 7 nAChR antagonist (Fig. 7B), and 1  $\mu$ M DH $\beta$ E, an  $\alpha$ 4 $\beta$ 2 antagonist (Fig. 7C). Treatment with the same concentrations of these antagonists or nicotine alone did not affect neurotoxicity. Nicotine-induced neuroprotection was therefore shown to occur via nAChRs, at least through  $\alpha$ 7 and  $\alpha$ 4 $\beta$ 2 receptors. Also, RT-PCR (Fig.

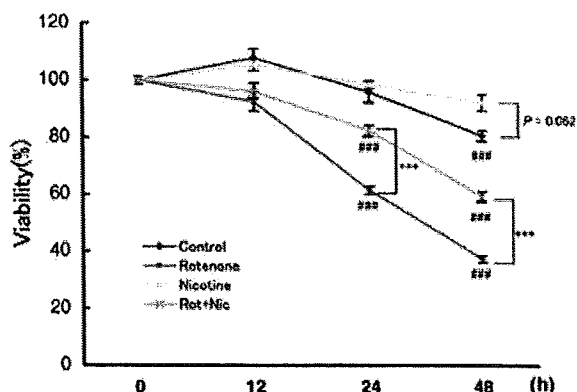


Fig. 5. Time course analysis of rotenone toxicity and nicotinic neuroprotection for TH-positive neurons, standardized by the number of control 0 hr. Both effects were shown after 24 hr since compounds were administered. Rotenone, rotenone 100 nM; Nicotine, nicotine 100  $\mu$ M; Rot+Nic, simultaneous administration of rotenone 100 nM and nicotine 100  $\mu$ M. Two-way factorial ANOVA was used for statistical analysis, followed by Bonferroni's multiple comparison test. Each value is the mean  $\pm$  SEM,  $n = 8$ ,  $###P < 0.001$  vs. control 0 hr,  $+++P < 0.001$  vs. rotenone 24 hr,  $***P < 0.001$  vs. rotenone 48 hr.

7D) showed that mRNA of nAChRs subunits was expressed in rat mesencephalic cells. These results are relevant to the previous report that  $\alpha$ 7 and  $\alpha$ 4 $\beta$ 2 nAChRs had biological activity in dopaminergic neurons in the midbrain (Champtiaux et al., 2003).

#### Nicotine-induced PI3K-Akt/PKB Pathway-activated Survival Activity of Dopaminergic Neurons

LY294002, a PI3K inhibitor inhibited nicotinic neuroprotection (Fig. 8A). Also triciribine, an Akt/PKB inhibitor, had the same effect (Fig. 8B). It is therefore likely that nicotine could activate the PI3K-Akt/PKB pathway or pathways and increased survival of mesencephalic dopaminergic cells against rotenone-induced cell death.

#### DISCUSSION

Rotenone works as a mitochondrial complex I inhibitor. Acute lethal doses of rotenone eliminate the mitochondrial respiratory system of the cell, resulting in an anoxic status that immediately causes cell death. At sublethal doses, it causes partial inhibition of mitochondrial complex I, and in this situation mitochondrial dysfunction leads to increased oxidative stress, decreased ATP production, increased aggregation of unfolded proteins, and then activated apoptotic pathway or pathways that result in cell death (Betarbet et al., 2000), resembling DA neurodegeneration in PD. Our data in vivo suggest that nicotine attenuated dopaminergic neuronal death of orally rotenone-treated PD model mice. It was relevant to the reports about the forebrain of rat models

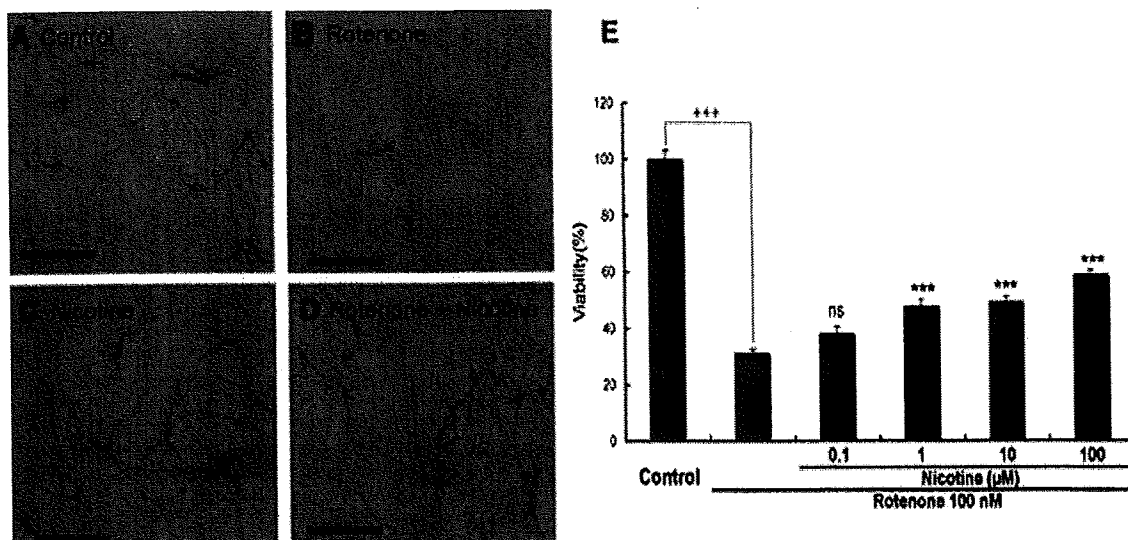


Fig. 6. Effect of nicotine on TH-positive neurons. Nicotine showed dose-dependent neuroprotection for dopaminergic neurons. A–D: Representative findings of each group of dopaminergic neurons. **A**: Control. **B**: Rotenone 100 nM. **C**: Nicotine 100 μM. **D**: Rotenone and nicotine added simultaneously for 48 hr. Scale bar = 200 μm. **E**: Statistical analysis of the viability of TH-positive cells, standardized by the number of control. Each value is the mean ± SEM,  $n = 8$ , \*\*\* $P < 0.001$  vs. rotenone 100 nM, +++ $P < 0.001$ .

(Cormier et al., 2003), as well as about 6-OHDA models (Visanji et al., 2006). Our orally rotenone-treated mouse model showed motor deficits, dopaminergic cell death in the substantia nigra, nerve terminal/axonal loss in the striatum. These findings are relevant to some previous reports about rotenone PD models (Schmidt and Alam, 2006; Ravenstijn et al., 2008). However, some failed to make animal PD models by rotenone (Lapointe et al., 2004; Höglinger et al., 2006). Although the mechanism is unclear, these inconsistencies may arise from the differences in animal species or mode of compound delivery (Quik et al., 2007b). Our data suggest that nicotinic protection might be more remarkable in cell bodies than in axon or nerve terminals. That was relevant to the previous reports about paraquat-induced (Khawaja et al., 2007) or MPTP-induced (Parain et al., 2003) mouse models, both mitochondrial complex I inhibitors, and rotarod treadmill test was reported to be useful for evaluating motor deficits in MPTP-treated mouse models of parkinsonism (Rozas et al., 1998).

The present data showed nicotinic neuroprotection was via nAChRs, and RT-PCR suggested that both  $\alpha 7$  and  $\alpha 4\beta 2$  nAChRs expressed on rat mesencephalic cells, whether they were on neurons or not. A previous report about the protective effect of nicotine against neurotoxicity suggested that a non- $\alpha 7$  receptor was involved (Jeyarasasingam et al., 2002). Our data showed that both  $\alpha 7$  and  $\alpha 4\beta 2$  receptors had relationships with neuroprotection. We have previously shown that neuronal  $\alpha 7$  nAChR stimulation appeared to activate the PI3K-Akt/

PKB pathway or pathways, leading to induced expression of antiapoptotic B cell lymphoma protein—mediating neuronal survival in  $A\beta$ -potentiated glutamate-induced neurotoxicity (Kihara et al., 2001). On the other hand, neuronal  $\alpha 4\beta 2$  nAChR stimulation causes DA release (Champtiaux et al., 2003), and our data showed the neuroprotective effect also occurred via  $\alpha 4\beta 2$  nAChRs, so the mechanism of neuroprotection could vary for different receptor subclasses. In addition, we have also shown the protective effect of dopamine D2 receptor agonists in cortical neurons via the PI3K cascade (Kihara et al., 2002). Also other nAChR subclasses were reported to be protective (Visanji et al., 2006), and nAChR agonists were protective. Previously it was reported that  $\alpha 4\beta 2$  nAChR stimulation might improve behavior of PD models (O'Neill et al., 2002), and epibatidine protected bovine chromaffin cells against rotenone-induced toxicity (Egea et al., 2007). We could not examine the effect of  $\alpha 6\beta 2$  nAChR stimulation, but it was reported to be neuroprotective (Quik and McIntosh, 2006). Further studies should be needed to assess other nAChRs by using other nAChR agonists or nicotinic components.

Our primary cultures contained not only neuronal cells but also glial cells, so glial cells may also be partly responsible for nicotinic neuroprotection. Microglial cells have  $\alpha 7$  nAChRs whose stimulation reduced the release of cytotoxic cytokines such as TNF $\alpha$  (Suzuki et al., 2006) and then decreased the activity of neuronal NF- $\kappa$ B (Liu et al., 2007). Chronically nicotine-treated rats might have NGF up-regulation in astrocytes of the

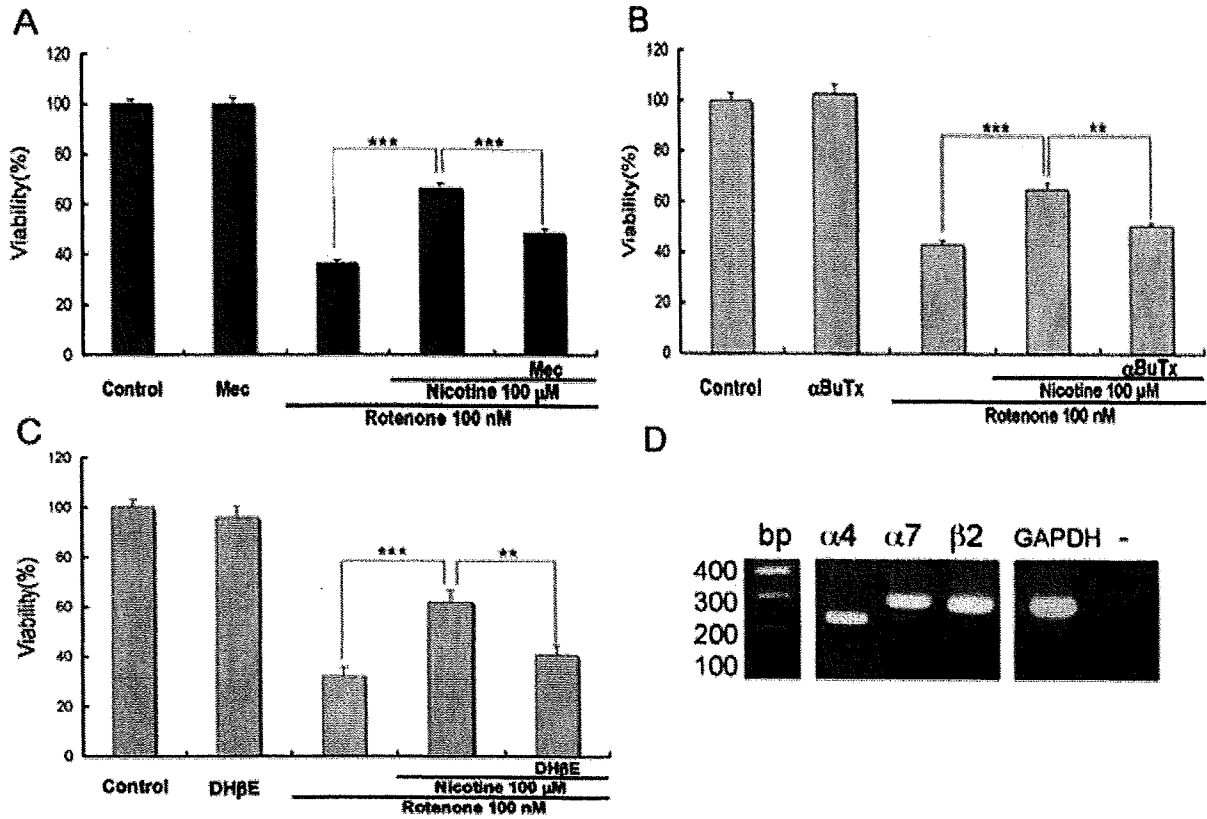


Fig. 7. A–C: Simultaneous administration of nicotinic acetylcholine receptor (nAChR) antagonists. Each antagonist blocked nicotinic neuroprotection, so it was suggested receptor-mediated. **A:** Mec, mecamylamine 100  $\mu$ M, a broad-spectrum antagonist of nAChRs. **B:**  $\alpha$ BuTx,  $\alpha$ -bungarotoxin 100 nM, an  $\alpha$ 7 nAChR antagonist. **C:** DH $\beta$ E, dihydro- $\beta$ -erythroidine 1  $\mu$ M, an  $\alpha$ 4 $\beta$ 2 nAChR antagonist. Each value is the mean  $\pm$  SEM,  $n = 8$ , \*\*\* $P < 0.01$ , \*\*\*\* $P < 0.001$ . **D:** Representa-

tive expression of mRNA for subunits of nAChRs in cultures of rat mesencephalic cells (day 8), RT-PCR products on an ethidium-bromide-stained gel. bp, number of base pairs; GAPDH, glyceraldehyde-3-phosphate dehydrogenase, which served as the internal control; -, negative control. Expression of mRNA for each  $\alpha$ 4,  $\alpha$ 7 and  $\beta$ 2 subunit was remarkable. Paired primers used were indicated in Table I. The same results were obtained three times.

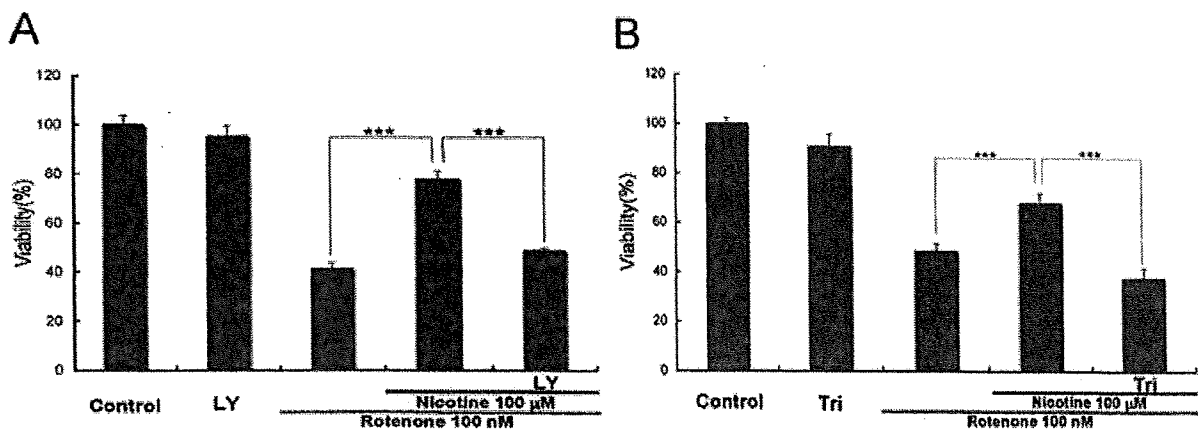


Fig. 8. Effects of the inhibitors of the PI3K-Akt/PKB pathway. Inhibition of either PI3K or Akt/PKB suppressed neuroprotective effect of nicotine. **A:** LY, LY294002 10  $\mu$ M, an inhibitor of PI3K. **B:** Tri, triciribine 1  $\mu$ M, an inhibitor of Akt/PKB. Each value is the mean  $\pm$  SEM,  $n = 8$ , \*\*\* $P < 0.001$ .

frontoparietal cortex (Martínez-Rodríguez et al., 2003). Nicotine decreased the number of activated microglial cells and TNF $\alpha$  and then protected dopaminergic neurons of MPTP-treated mice (Park et al., 2007). So glial cells may also play a role for the mechanism of the neuroprotection we have seen in the present study. We should also analyze glial neuroprotection by nicotine.

As mentioned above, other compounds that stimulate nAChRs show functional improvement in nonhuman primates (Quik et al., 2006, 2007a) and have neuroprotective effects are now on clinical trial, but the results were controversial. For example, SIB-1508Y, an  $\alpha 4\beta 2$  nAChR agonist, failed to improve symptoms of PD (Parkinson Study Group, 2006). Some cholinesterase inhibitors, for example, galantamine is an allosteric potentiating ligand (Santos et al., 2002) and stimulates cholinergic neurons in the nucleus basalis of Meynert, were reported to be effective for cognitive dysfunction of PD with dementia and Lewy body disease, a parkinsonism with hallucination and fluctuating dementia (Burn et al., 2006; Mentis et al., 2006, Miyasaki et al., 2006), but there may be deterioration of motor dysfunction due to simultaneous muscarinic acetylcholine receptor stimulation in the striatum. Thus, further analysis of glial neuroprotective effect by nicotine may be needed.

In conclusion, by stimulating nAChRs, the PI3K-Akt/PKB pathway or pathways could be activated to suppress dopaminergic cell death induced by rotenone. Additionally, chronic oral administration of rotenone induced motor deficits and nigrostriatal dopaminergic neurodegeneration in C57/BL6 mice, and nicotine attenuated both of them. These results suggest that derivatives of nicotine or agents that stimulate nAChRs may be useful for neuroprotective therapies targeting PD. In addition, rotenone-treated mice may be useful for understanding the mechanisms of dopaminergic cell death and may serve as a model of environmental factors involved in PD pathogenesis.

#### ACKNOWLEDGMENTS

This work was supported in part by the 21st Century Center of Excellence (COE) Program, the grants from Ministry of Education, Culture, Sports, Science and Technology of Japan, Japan Society for the Promotion of Science, Ministry of Health, Labour and Welfare of Japan, Smoking Research Foundation, and Philip Morris USA Inc. and Philip Morris International.

We thank to Megumi Asada-Utsugi, School of Health Sciences, Faculty of Medicine, Kyoto University, for contributing to the RT-PCR analysis.

#### REFERENCES

- Akaike A, Tamura Y, Yokota T, Shimohama S, Kimura J. 1994. Nicotine-induced protection of cultured cortical neurons against N-methyl-D-aspartate receptor-mediated glutamate cytotoxicity. *Brain Res* 644:181–187.
- Baquet Z, Bickford P, Jones K. 2005. Brain-derived neurotrophic factor is required for the establishment of the proper number of dopaminergic neurons in the substantia nigra pars compacta. *J Neurosci* 25:6251–6259.
- Betarbet R, Sherer T, MacKenzie G, Garcia-Osuna M, Panov A, Greenamyre J. 2000. Chronic systemic pesticide exposure reproduces features of Parkinson's disease. *Nat Neurosci* 3:1301–1306.
- Burn D, Emre M, McKeith I, De Deyn P, Aarsland D, Hsu C, Lane R. 2006. Effects of rivastigmine in patients with and without visual hallucinations in dementia associated with Parkinson's disease. *Mov Disord* 21:1899–1907.
- Champtiaux N, Gotti C, Cordero-Erausquin M, David D, Przybylski C, Léna C, Clementi F, Moretti M, Rossi F, Le Novère N, McIntosh J, Gardier A, Changeux J. 2003. Subunit composition of functional nicotinic receptors in dopaminergic neurons investigated with knock-out mice. *J Neurosci* 23:7820–7829.
- Chomczynski P, Sacchi N. 1987. Single-step method of RNA isolation by acid guanidinium thiocyanate-phenol-chloroform extraction. *Anal Biochem* 162:156–159.
- Cormier A, Morin C, Zini R, Tillement J, Lagrue G. 2003. Nicotine protects rat brain mitochondria against experimental injuries. *Neuropharmacology* 44:642–652.
- De Reuck J, De Weweire M, Van Maele G, Santens P. 2005. Comparison of age of onset and development of motor complications between smokers and non-smokers in Parkinson's disease. *J Neurol Sci* 231:35–39.
- Du F, Li R, Huang Y, Li X, Le W. 2005. Dopamine D3 receptor-preferring agonists induce neurotrophic effects on mesencephalic dopamine neurons. *Eur J Neurosci* 22:2422–2430.
- Dunnett S, Björklund A. 1999. Prospects for new restorative and neuroprotective treatments in Parkinson's disease. *Nature* 399:A32–A39.
- Egea J, Rosa A, Cuadrado A, García A, López M. 2007. Nicotinic receptor activation by epibatidine induces heme oxygenase-1 and protects chromaffin cells against oxidative stress. *J Neurochem* 102:1842–1852.
- Fujita M, Ichise M, Zoghbi S, Liow J, Ghose S, Vines D, Sangare J, Lu J, Cropley V, Iida H, Kim K, Cohen R, Bara-Jimenez W, Ravina B, Innis R. 2006. Widespread decrease of nicotinic acetylcholine receptors in Parkinson's disease. *Ann Neurol* 59:174–177.
- Grinevich V, Letchworth S, Lindenberger K, Menager J, Mary V, Sadiieva K, Buhlman L, Bohme G, Pradier L, Benavides J, Lukas R, Bencherif M. 2005. Heterologous expression of human  $\alpha 6\beta 4\beta 3\alpha 5$  nicotinic acetylcholine receptors: binding properties consistent with their natural expression require quaternary subunit assembly including the  $\alpha 5$  subunit. *J Pharmacol Exp Ther* 312:619–626.
- Gundersen H, Bendtsen T, Korbo L, Marcussen N, Møller A, Nielsen K, Nyengaard J, Pakkenberg B, Sørensen F, Vesterby A. 1988. Some new, simple and efficient stereological methods and their use in pathological research and diagnosis. *APMIS* 96:379–394.
- Höglinger G, Oertel W, Hirsch E. 2006. The rotenone model of parkinsonism—the five years inspection. *J Neural Transm Suppl* 70:269–272.
- Inden M, Kitamura Y, Takeuchi H, Yanagida T, Takata K, Kobayashi Y, Taniguchi T, Yoshimoto K, Kaneko M, Okuma Y, Taira T, Ariga H, Shimohama S. 2007. Neurodegeneration of mouse nigrostriatal dopaminergic system induced by repeated oral administration of rotenone is prevented by 4-phenylbutyrate, a chemical chaperone. *J Neurochem* 101:1491–1504.
- Iravani M, Haddon C, Cooper J, Jenner P, Schapira A. 2006. Pramipexole protects against MPTP toxicity in non-human primates. *J Neurochem* 96:1315–1321.
- Jeyarasasingam G, Tompkins L, Quik M. 2002. Stimulation of non- $\alpha 7$  nicotinic receptors partially protects dopaminergic neurons from 1-methyl-4-phenylpyridinium-induced toxicity in culture. *Neuroscience* 109:275–285.
- Kagitani F, Uchida S, Hotta H, Sato A. 2000. Effects of nicotine on blood flow and delayed neuronal death following intermittent transient ischemia in rat hippocampus. *Jpn J Physiol* 50:585–595.

- Khawaja M, McCormack A, McIntosh J, Di Monte D, Quik M. 2007. Nicotine partially protects against paraquat-induced nigrostriatal damage in mice; link to  $\alpha 6 \beta 2^*$  nAChRs. *J Neurochem* 100:180–190.
- Kihara T, Shimohama S, Sawada H, Kimura J, Kume T, Kochiyama H, Maeda T, Akaïke A. 1997. Nicotinic receptor stimulation protects neurons against beta-amyloid toxicity. *Ann Neurol* 42:159–163.
- Kihara T, Shimohama S, Sawada H, Honda K, Nakamizo T, Shibasaki H, Kume T, Akaïke A. 2001.  $\alpha 7$  nicotinic receptor transduces signals to phosphatidylinositol 3-kinase to block Abeta-amyloid-induced neurotoxicity. *J Biol Chem* 276:13541–13546.
- Kihara T, Shimohama S, Sawada H, Honda K, Nakamizo T, Kanki R, Yamashita H, Akaïke A. 2002. Protective effect of dopamine D2 agonists in cortical neurons via the phosphatidylinositol 3 kinase cascade. *J Neurosci Res* 70:274–282.
- Lapointe N, St-Hilaire M, Martinoli M, Blanchet J, Gould P, Rouillard C, Cicchetti F. 2004. Rotenone induces non-specific central nervous system and systemic toxicity. *FASEB J* 18:717–719.
- Liu Q, Zhang J, Zhu H, Qin C, Chen Q, Zhao B. 2007. Dissecting the signaling pathway of nicotine-mediated neuroprotection in a mouse Alzheimer disease model. *FASEB J* 21:61–73.
- Martínez-Rodríguez R, Toledano A, Alvarez M, Turégano L, Colman O, Rosés P, Gómez de Segura I, De Miguel E. 2003. Chronic nicotine administration increases NGF-like immunoreactivity in frontoparietal cerebral cortex. *J Neurosci Res* 73:708–716.
- Mann V, Cooper J, Krige D, Daniel S, Schapira A, Marsden C. 1992. Brain, skeletal muscle and platelet homogenate mitochondrial function in Parkinson's disease. *Brain* 115(Pt 2):333–342.
- Mentis M, Delalot D, Naqvi H, Gordon M, Gudesblatt M, Edwards C, Donatelli L, Dhawan V, Eidelberg D. 2006. Anticholinesterase effect on motor kinematic measures and brain activation in Parkinson's disease. *Mov Disord* 21:549–555.
- Miyasaki J, Shannon K, Voon V, Ravina B, Kleiner-Fisman G, Anderson K, Shulman L, Gronseth G, Weiner W; Quality Standards Subcommittee of the American Academy of Neurology. 2006. Practice Parameter: evaluation and treatment of depression, psychosis, and dementia in Parkinson disease (an evidence-based review): report of the Quality Standards Subcommittee of the American Academy of Neurology. *Neurology* 66:996–1002.
- Mizuno Y, Yoshino H, Ikebe S, Hattori N, Kobayashi T, Shimoda-Matsubayashi S, Matsumine H, Kondo T. 1998. Mitochondrial dysfunction in Parkinson's disease. *Ann Neurol* 44(3 Suppl 1):S99–S109.
- Morens D, Grandinetti A, Reed D, White L, Ross G. 1995. Cigarette smoking and protection from Parkinson's disease: false association or etiologic clue? *Neurology* 45:1041–1051.
- Nakamizo T, Kawamata J, Yamashita H, Kanki R, Kihara T, Sawada H, Akaïke A, Shimohama S. 2005. Stimulation of nicotinic acetylcholine receptors protects motor neurons. *Biochem Biophys Res Commun* 330:1285–1289.
- O'Neill M, Murray T, Lakies V, Visanji N, Duty S. 2002. The role of neuronal nicotinic acetylcholine receptors in acute and chronic neurodegeneration. *Curr Drug Targets CNS Neurol Disord* 1:399–411.
- Parain K, Hapdey C, Rousselet E, Marchand V, Dumery B, Hirsch E. 2003. Cigarette smoke and nicotine protect dopaminergic neurons against the 1-methyl-4-phenyl-1,2,3,6-tetrahydropyridine Parkinsonian toxin. *Brain Res* 984:224–232.
- Park H, Lee P, Ahn Y, Choi Y, Lee G, Lee D, Chung E, Jin B. 2007. Neuroprotective effect of nicotine on dopaminergic neurons by anti-inflammatory action. *Eur J Neurosci* 26:79–89.
- Parker W Jr, Boyson S, Parks J. 1989. Abnormalities of the electron transport chain in idiopathic Parkinson's disease. *Ann Neurol* 26:719–723.
- Parkinson Study Group. 2006. Randomized placebo-controlled study of the nicotinic agonist SIB-1508Y in Parkinson disease. *Neurology* 66:408–410.
- Quik M. 2004. Smoking, nicotine and Parkinson's disease. *Trends Neurosci* 27:561–568.
- Quik M, McIntosh J. 2006. Striatal  $\alpha 6^*$  nicotinic acetylcholine receptors: potential targets for Parkinson's disease therapy. *J Pharmacol Exp Ther* 316:481–489.
- Quik M, Chen L, Parameswaran N, Xie X, Langston J, McCallum S. 2006. Chronic oral nicotine normalizes dopaminergic function and synaptic plasticity in 1-methyl-4-phenyl-1,2,3,6-tetrahydropyridine-lesioned primates. *J Neurosci* 26:4681–4689.
- Quik M, Cox H, Parameswaran N, O'Leary K, Langston J, Di Monte D. 2007a. Nicotine reduces levodopa-induced dyskinesias in lesioned monkeys. *Ann Neurol* 62:588–596.
- Quik M, O'Neill M, Perez X. 2007b. Nicotine neuroprotection against nigrostriatal damage: importance of the animal model. *Trends Pharmacol Sci* 28:229–235.
- Ravenstijn P, Merlini M, Hameetman M, Murray T, Ward M, Lewis H, Ball G, Mottart C, de Ville de Goyet C, Lemarchand T, van Belle K, O'Neill M, Danhof M, de Lange E. 2008. The exploration of rotenone as a toxin for inducing Parkinson's disease in rats, for application in BBB transport and PK-PD experiments. *J Pharmacol Toxicol Methods* 57:114–130.
- Rozas G, Liste I, Guerra M, Labandeira-Garcia J. 1998. Sprouting of the serotonergic afferents into striatum after selective lesion of the dopaminergic system by MPTP in adult mice. *Neurosci Lett* 245:151–154.
- Santos M, Alkondon M, Pereira E, Aracava Y, Eisenberg H, Maelicke A, Albuquerque E. 2002. The nicotinic allosteric potentiating ligand galantamine facilitates synaptic transmission in the mammalian central nervous system. *Mol Pharmacol* 61:1222–1234.
- Sawada H, Kohno R, Kihara T, Izumi Y, Sakka N, Ibi M, Nakanishi M, Nakamizo T, Yamakawa K, Shibasaki H, Yamamoto N, Akaïke A, Inden M, Kitamura Y, Taniguchi T, Shimohama S. 2004. Proteasome mediates dopaminergic neuronal degeneration, and its inhibition causes alpha-synuclein inclusions. *J Biol Chem* 279:10710–10719.
- Schapira A. 2006. Etiology of Parkinson's disease. *Neurology* 66(10 Suppl 4):S10–S23.
- Schmidt W, Alam M. 2006. Controversies on new animal models of Parkinson's disease pro and con: the rotenone model of Parkinson's disease (PD). *J Neural Transm Suppl* 70:273–276.
- Shimohama S, Greenwald D, Shafron D, Akaïke A, Maeda T, Kaneko S, Kimura J, Simpkins C, Day A, Meyer E. 1998. Nicotinic  $\alpha 7$  receptors protect against glutamate neurotoxicity and neuronal ischemic damage. *Brain Res* 779:359–363.
- Shimohama S, Sawada H, Kitamura Y, Taniguchi T. 2003. Disease model: Parkinson's disease. *Trends Mol Med* 9:360–365.
- Suzuki T, Hide I, Matsubara A, Hama C, Harada K, Miyano K, Andri M, Matsubayashi H, Sakai N, Kohsaka S, Inoue K, Nakata Y. 2006. Microglial  $\alpha 7$  nicotinic acetylcholine receptors drive a phospholipase C/IP3 pathway and modulate the cell activation toward a neuroprotective role. *J Neurosci Res* 83:1461–1470.
- Visanji N, O'Neill M, Duty S. 2006. Nicotine, but neither the  $\alpha 4$ - $\beta 2$  ligand RJR2403 nor an  $\alpha 7$  nAChR subtype selective agonist, protects against a partial 6-hydroxydopamine lesion of the rat median forebrain bundle. *Neuropharmacology* 51:506–516.
- West M, Slomianka L, Gundersen J. 1991. Unbiased stereological estimation of the total number of neurons in the subdivisions of the rat hippocampus using the optical fractionator. *Anat Rec* 231:482–497.
- Wirdefeldt K, Gatz M, Pawitan Y, Pedersen N. 2005. Risk and protective factors for Parkinson's disease: a study in Swedish twins. *Ann Neurol* 57:27–33.
- Xie Y, Bezdard E, Zhao B. 2005. Investigating the receptor-independent neuroprotective mechanisms of nicotine in mitochondria. *J Biol Chem* 280:32405–32412.



## N-cadherin-based adhesion enhances A $\beta$ release and decreases A $\beta_{42/40}$ ratio

Kengo Uemura,\* Christina M. Lill,† Mary Banks,† Megumi Asada,‡ Nobuhisa Aoyagi,\* Koichi Ando,\* Masakazu Kubota,‡ Takeshi Kihara,§ Takaaki Nishimoto,§ Hachiro Sugimoto,§ Ryosuke Takahashi,\* Bradley T. Hyman,† Shun Shimohama,¶ Oksana Berezovska† and Ayae Kinoshita‡

\*Department of Neurology, Graduate School of Medicine, Kyoto University, Kyoto, Japan

†Alzheimer Research Unit, Massachusetts General Hospital, Charlestown, Massachusetts, USA

‡School of Health Sciences, Graduate School of Medicine, Kyoto University, Kyoto, Japan

§Department of Neuroscience for Drug Discovery, Graduate School of Pharmaceutical Sciences, Kyoto University, Kyoto, Japan

¶Department of Neurology, Sapporo Medical University, Sapporo, Japan

### Abstract

In neurons, Presenilin 1 (PS1)/ $\gamma$ -secretase is located at the synapses, bound to N-cadherin. We have previously reported that N-cadherin-mediated cell–cell contact promotes cell-surface expression of PS1/ $\gamma$ -secretase. We postulated that N-cadherin-mediated trafficking of PS1 might impact synaptic PS1-amyloid precursor protein interactions and A $\beta$  generation. In the present report, we evaluate the effect of N-cadherin-based contacts on A $\beta$  production. We demonstrate that stable expression of N-cadherin in Chinese hamster ovary cells, expressing the Swedish mutant of human amyloid precursor protein leads to enhanced secretion of A $\beta$  in the

medium. Moreover, N-cadherin expression decreased A $\beta_{42/40}$  ratio. The effect of N-cadherin expression on A $\beta$  production was accompanied by the enhanced accessibility of PS1/ $\gamma$ -secretase to amyloid precursor protein as well as a conformational change of PS1, as demonstrated by the fluorescence lifetime imaging technique. These results indicate that N-cadherin-mediated synaptic adhesion may modulate A $\beta$  secretion as well as the A $\beta_{42/40}$  ratio via PS1/N-cadherin interactions.

**Keywords:** Alzheimer's disease, amyloid  $\beta$ , N-cadherin, presenilin 1, synapse.

*J. Neurochem.* (2009) **108**, 350–360.

Amyloid  $\beta$  (A $\beta$ ) peptides are the major components of senile plaques, a pathological hallmark of Alzheimer's disease (AD), and are generated by the intramembranous cleavage of the amyloid precursor protein (APP) C-terminal fragment by Presenilin 1 (PS1)/ $\gamma$ -secretase (De Strooper *et al.* 1998). PS1 is a multitransmembrane protein with a 30-kDa N-terminal fragment (NT), a 20-kDa C-terminal fragment (CT) and a large cytoplasmic loop domain (Thinakaran *et al.* 1996). Most of the PS1 mutations associated with familial AD (FAD) are known to increase the ratio of A $\beta_{42}$ –A $\beta_{40}$  (A $\beta_{42/40}$  ratio), thereby increasing the more aggregation-prone A $\beta_{42}$  relative to A $\beta_{40}$  (Citron *et al.* 1997), which is considered at present to be an important molecular background of FAD pathogenesis. Using fluorescence lifetime imaging microscopy (FLIM), we have previously demonstrated that FAD-linked mutations in PS1 change the spatial relationship between PS1 NT and CT, increasing proximity of the two

epitopes (Berezovska *et al.* 2005). This effect was contrary to that observed after the treatment with A $\beta_{42}$ -lowering non-steroidal anti-inflammatory drugs (NSAIDs) which leads to the opposite conformational effect with PS1 NT and CT further apart (Leo *et al.* 2004). These findings suggested that

Received June 20, 2008; revised manuscript received September 10, 2008; accepted October 20, 2008.

Address correspondence and reprint requests to Ayae Kinoshita, School of Health Sciences, Graduate School of Medicine, Kyoto University, 53 Shogoinawahara-cho, Sakyo-ku, Kyoto 606–8507, Japan. E-mail: akinoshita@bs.med.kyoto-u.ac.jp

**Abbreviations used:** AD, Alzheimer's disease; APP, amyloid precursor protein; APPSw, APP Swedish mutant; A $\beta$ , amyloid  $\beta$ ; CHO, Chinese hamster ovary; CT, C-terminal fragment; FAD, familial AD; FLIM, fluorescence lifetime imaging technique; FRET, fluorescence resonance energy transfer; NSAIDs, nonsteroidal anti-inflammatory drugs; NT, N-terminal fragment; PS1, presenilin 1.

conformational change in PS1 because of mutations or to allosteric influences provides a possible structural basis for altered A $\beta_{42/40}$  ratio.

In neurons, PS1 binds to  $\beta$ -catenin and N-cadherin at the synapse (Georgakopoulos *et al.* 1999). N-cadherin is essential for forming synaptic contact as well as for specific neuronal function such as synaptic plasticity (Bozdagi *et al.* 2000; Togashi *et al.* 2002). Accumulating evidence suggests that A $\beta$  release may be regulated by synaptic activity (Kamenetz *et al.* 2003; Cirrito *et al.* 2005; Lesne *et al.* 2005). However, it remains largely unknown how PS1/ $\gamma$ -secretase-mediated APP cleavage is regulated by synaptic activity. We have recently demonstrated that N-cadherin promotes the cell-surface expression of PS1/ $\gamma$ -secretase via direct interaction with PS1 loop domain (Uemura *et al.* 2007). This result indicated that N-cadherin may recruit PS1/ $\gamma$ -secretase to synaptic sites. Thus, we hypothesize that N-cadherin-based synaptic adhesion may influence A $\beta$  production.

Here, we demonstrate that stable expression of N-cadherin in cadherin-deficient Chinese hamster ovary (CHO) cells expressing human APP Swedish mutant (APPSw) enhances the A $\beta$  levels in the medium, possibly by increasing the accessibility of APP to PS1/ $\gamma$ -secretase. Moreover, N-cadherin expression induces a structural change in PS1, similar to that previously observed to accompany NSAID-induced decrease in A $\beta_{42/40}$  ratio. These results indicate that N-cadherin-PS1 interactions may modulate A $\beta$  production at the synapse, providing novel insight into AD pathophysiology.

## Materials and methods

### Plasmid constructs

The construction of the expression vector encoding human N-cadherin tagged with HA at its C-terminus was described previously (Uemura *et al.* 2006b). The construction of the plasmid, expressing wtPS1 and the production of deletion mutant of PS1 ( $\Delta$ 340-350PS1), which is unable to interact with N-cadherin was described previously (Uemura *et al.* 2007). Precise cloning of all reading frame was verified by sequencing. The expression vector of APP-GFP was described elsewhere (Kinoshita *et al.* 2002). The original PS1-GFP (in the loop) construct was a generous gift from Dr. Kaether (Ludwig-Maximilians University, Germany) and was created by introducing a Not1-GFP-Not1 between codon 351 and 352 of the cytoplasmic loop of human PS1. The RFP fragment with Not1 restriction sites at 5' and 3' ends was generated by PCR and GFP was replaced by RFP.

### Cell culture and transfection

Chinese hamster ovary cells were maintained in Dulbecco's modified Eagle's medium/F12 (Invitrogen, Carlsbad, CA, USA) supplemented with 10% fetal bovine serum. Transient transfection of wtPS1, PS1 mutant ( $\Delta$ 340-350PS1) and N-cadherin into cells were achieved by lipofection method, using Lipofectamine 2000 (Invitrogen) according to the manufacturer's instructions. CHO cells, stably expressing Swedish (K670/M671->N/L) mutant human

APP695 (APPSw-CHO cells) and CHO cells stably expressing both Swedish mutant APP and human N-cadherin (APPSw/Ncad-CHO cells) were obtained as described elsewhere (Uemura *et al.* 2007). Primary cultured neurons were obtained from the hippocampus of fetal rats (17–19 days gestation) as described previously (Uemura *et al.* 2006a). Cultures were incubated in Eagle's Minimum Essential Medium supplemented with 10% fetal calf serum or 10% horse serum.

### Antibodies and chemical reagents

Mouse monoclonal anti-N-cadherin C-terminus and anti- $\beta$ -catenin antibodies are obtained from Transduction Laboratories. Mouse monoclonal anti- $\beta$ -actin antibody, mouse monoclonal anti-N-cadherin N-terminus antibody (N-cadherin neutralizing antibody, GC-4), rabbit polyclonal anti-nicastrin antibody, rabbit polyclonal anti-APP C-terminus antibody and control normal mouse IgG are from Sigma (St Louis, MO, USA). Rabbit polyclonal anti-PS1 N-terminal fragment and control normal rabbit IgG were from Santa Cruz, Santa Cruz, CA, USA. Rabbit polyclonal anti-BACE1 antibody was from Calbiochem, San Diego, CA, USA. Rat monoclonal anti-PS1 N-terminal fragment antibody was from Chemicon, Temecula, CA, USA. Alexa Fluor 546 goat anti-mouse IgG, Alexa Fluor 546-phalloidin, and Alexa Fluor 488 goat anti-rabbit IgG, and Cy3-anti-rabbit IgG were obtained from Molecular Probes, Eugene, OR, USA. Anti-mouse and rabbit horseradish peroxidase-conjugated secondary antibodies are from Amersham Biosciences, Piscataway, NJ, USA.

### Cell treatment by reagents

For the inhibition of N-cadherin-mediated cell-cell contact, cells were treated with 80  $\mu$ g/mL of N-cadherin-neutralizing antibody (GC-4) in OPTI-MEM for indicated period of time. Control cells were treated with an equal amount of normal mouse IgG.

### Western blot and immunoprecipitation

Preparation of protein samples, the western blot and immunoprecipitation analysis were carried out as described elsewhere (Uemura *et al.* 2007).

### Immunostaining

The samples for immunostaining were prepared as described elsewhere (Uemura *et al.* 2007). After fixation, samples were examined using a laser scanning confocal microscopy, LSM 510 META (Zeiss, Jena, Germany) or BZ-9000 fluorescent microscopy (KEYENCE).

### Measurement of BACE1 activity

$\beta$ -secretase activity was measured by using  $\beta$ -secretase activity kit (R&D systems). Briefly,  $2.5 \times 10^5$  cells of APPSw-CHO cells or APPSw/Ncad-CHO cells were plated in 3.5 cm dish and cultured overnight. Cells were collected and lysed by adding 500  $\mu$ L of 1 $\times$  cell extraction buffer. Protein concentration of each cell lysate was determined by the Bradford method (Uemura *et al.* 2003) and equal amount of protein was subjected to the  $\beta$ -secretase activity assay, according to the manufacturer's instruction.

### Fluorescence lifetime imaging microscopy assay

To analyze the PS1 conformation and/or PS1-APP interactions in intact cells expressing or not expressing N-cadherin, the APPSw-

CHO or APPSw/Ncad-CHO cells were fixed and double-immunostained with corresponding antibodies labeled with Cy3 and Alexa 488 for the FLIM analysis. To monitor PS1 conformation, we used goat anti-PS1 NT and rabbit anti-PS1 CT antibodies from Sigma. For the analysis of PS1-APP interactions we used mouse anti-PS1 antibody raised against amino acids 267–378 in the major TM6-7 loop domain (Chemicon) and an antibody to APP CT (Sigma). The fluorescence lifetime of a donor fluorophore (Alexa 488) was measured as described previously (Berezovska *et al.* 2005). In order to confirm the N-cadherin-mediated cell adhesion effect on A $\beta$  production, we also examined the proximity between APP and PS1 in the presence of N-cadherin-neutralizing antibody (GC-4). For this blocking experiment, we modified the protocol for the FLIM assay since GC-4 is a mouse monoclonal antibody, which might cross-react the immunohistochemical results described above. We did two complementary FLIM experiments: (i) CHO cells stably expressing APPSw and N-cadherin were treated for 6 h with 80  $\mu$ g/mL of either anti-N-cadherin blocking antibody (GC-4) or normal IgG as a control. The cells were fixed and immunostained with antibodies against APP (rabbit anti-APP CT, Sigma) and PS1 (goat anti-PS1 NT, Sigma) for the FLIM analysis. (ii) The cells were transfected with C-terminally labeled APP-GFP and PS1-RFP (tagged in the TM6-7 loop region), treated with CG4 or IgG and the FLIM analysis was performed on the living cells.

#### Measurement of extracellular A $\beta$

A $\beta$  peptides produced by rat hippocampus primary neurons were measured by using Mouse/Rat Amyloid  $\beta$  (1–40) (N) Assay Kit (IBL, Gumbia, Japan). Primary neurons, cultured in 3.5 cm dish were washed once with OPTI-MEM and then incubated in OPTI-MEM for indicated periods of time. After incubation, the culture medium was collected, centrifugated at 600 g for 5 min, and the 100  $\mu$ L of the aliquot was used for the extracellular sample. A $\beta_{40}$  and A $\beta_{42}$  peptides produced by APPSw-CHO cells or APPSw/Ncad-CHO cells were measured by using Human  $\beta$  Amyloid (1–40) and (1–42) ELISA Kit (WAKO, Osaka, Japan), respectively.  $6 \times 10^5$  of APPSw-CHO cells or APPSw/Ncad-CHO cells cultured in 3.5 cm dish were washed once with OPTI-MEM and then incubated in OPTI-MEM for indicated period of time. After incubation, the culture medium was collected, centrifugated 600 g, 5 min, and the 100  $\mu$ L of the aliquot was used for measurement of extracellular A $\beta$ .

#### Statistical analysis

All values are given in means  $\pm$  SE. Comparisons were performed using a paired Student's *t*-test. For comparison of multiparametric analysis, one-way factorial ANOVA, followed by the *post hoc* analysis by Fisher's PLSD was used.  $p < 0.05$  was considered to indicate a significant difference.  $n = 4$  indicates four independent experiments.

## Results

### N-cadherin expression enhances A $\beta$ secretion and reduces A $\beta_{42/40}$ ratio

The purpose of our study is to define the effect of a synaptic adhesion molecule, N-cadherin, on A $\beta$  production by using biochemical (western blot and ELISA) and fluorescence

resonance energy transfer (FRET)-based FLIM assay. First, we determined whether stable expression of N-cadherin could enhance the production of A $\beta$ . To test this, CHO cells stably expressing Swedish (K670N/M671L) mutant human APP695 (APPSw-CHO cells) and CHO cells stably expressing both APPSw and human N-cadherin (APPSw/Ncad-CHO cells) were established. The expression levels of BACE1 and  $\gamma$ -secretase components were similar between APPSw-CHO and APPSw/Ncad-CHO cells (Fig. 1a). BACE1 activity was not significantly different between these cell lines (Figure 1b). Immunocytochemical analysis using anti-N-cadherin and anti-PS1 antibodies revealed colocalization of these proteins at the sites of cell–cell contact and at the cell surface [Fig. 1c–f, see also Uemura *et al.* (2007)], indicating that PS1/ $\gamma$ -secretase was recruited to the cell-surface upon formation of N-cadherin-based cell-cell contact.

Next, we compared the levels of A $\beta_{40}$  and A $\beta_{42}$  in the medium between APPSw-CHO and APPSw/Ncad-CHO cells. Both A $\beta_{40}$  (Fig. 2a) and A $\beta_{42}$  (Fig. 2b) levels were increased by stable expression of N-cadherin. Interestingly, the A $\beta_{42/40}$  ratio was significantly reduced in N-cadherin expressing cells (Fig. 2c). We established four independent clones of APPSw/Ncad-CHO cells, all of which produced significantly higher amounts of extracellular A $\beta_{40}$ , compared with the original APPSw-CHO cells (Fig. 2d). Moreover, in order to confirm that enhanced A $\beta$  secretion in APPSw/Ncad-CHO cells is specifically caused by the expression of N-cadherin, we used well-characterized N-cadherin-neutralizing antibody (GC-4) (De Wever *et al.* 2004) to inhibit N-cadherin-mediated contacts. The N-cadherin-neutralizing antibody inhibited the release of A $\beta_{40}$  from APPSw/Ncad-CHO cells (Fig. 2e, white columns), whereas it had no effect on APPSw-CHO cells (Fig. 2e, black columns). The level of A $\beta_{40}$  secreted from APPSw/Ncad-CHO cells after N-cadherin-neutralizing antibody treatment was similar to that of the original APPSw-CHO cells, indicating that the enhanced extracellular release of A $\beta$  from these cells was specifically caused by the N-cadherin expression. Next, to confirm the effect of N-cadherin expression on the metabolism of wild-type APP, we established CHO cell line, which expresses wild-type APP with (APPWt/Ncad-CHO cells) or without (APPWt-CHO cells) N-cadherin (Supporting information Fig. S1a). Both stable and transient expression of N-cadherin reduced A $\beta_{42/40}$  ratio in the background of wild-type APP expression. Thus, these results strongly suggest that N-cadherin influences wild-type as well as mutant APP metabolism (Supporting information Figure S1b–e).

### N-cadherin expression increases the accessibility of PS1/ $\gamma$ -secretase to its substrate APP

We have previously demonstrated by the FLIM assay that close association of PS1 and APP preferentially occurs in the

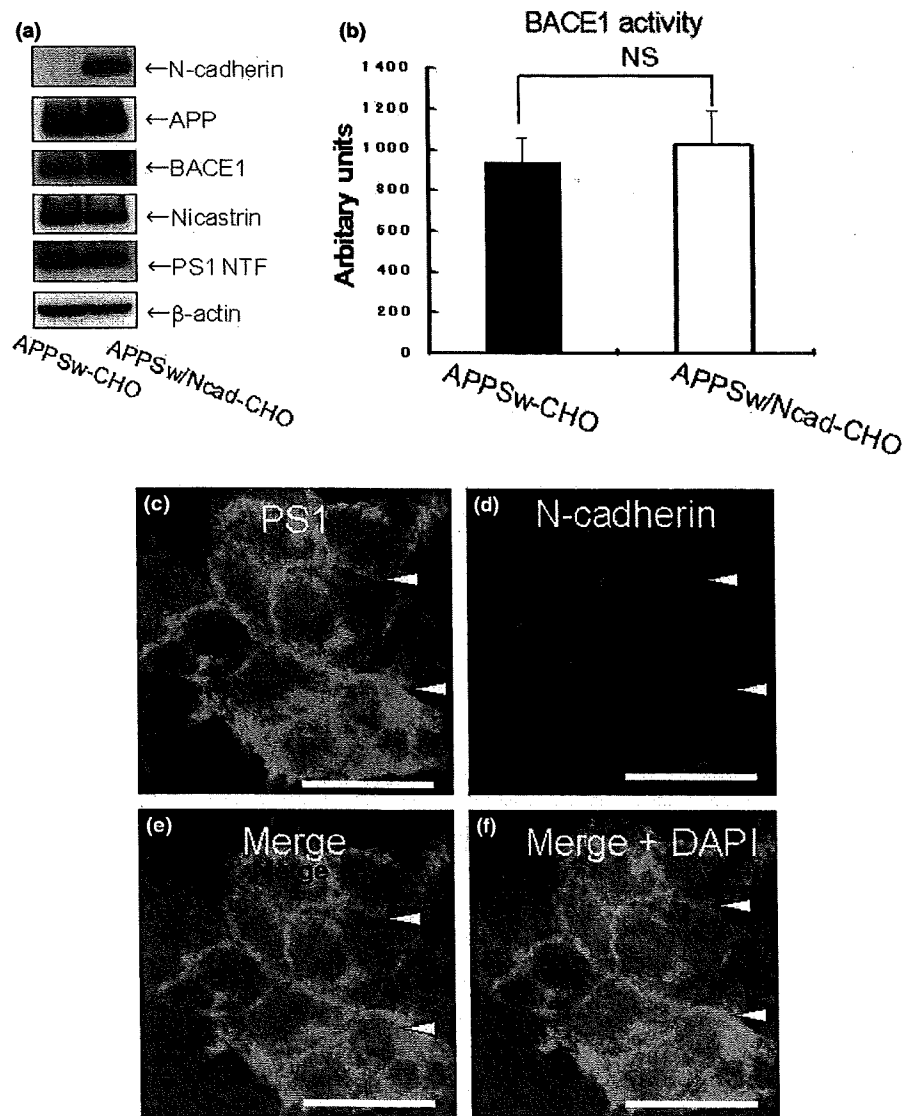


**Fig. 1** Characterization of APPSw/Ncad-CHO cells. (a) APPSw-CHO cells and APPSw/Ncad-CHO cells were analyzed by western blot. N-cadherin was expressed only in APPSw/Ncad-CHO cells. The expression levels of APP, BACE1, nicastrin, PS1 NT were similar in both cell lines. The bottom lane indicates the  $\beta$ -actin level, which was used as a loading control. (b) APPSw-CHO cells and APPSw/Ncad-CHO cells were lysed and  $\beta$ -secretase activity in the lysate was measured. No significant difference was found between these cell

lines ( $p = 0.15$ ,  $n = 4$ ). (c–f) APPSw/Ncad-CHO cells were immunostained with rabbit polyclonal anti-PS1 NT (c) and mouse monoclonal anti-N-cadherin antibodies (d). Merged image is shown in (e). Merged image with nuclear DAPI staining is shown in (f). The fixed samples were analyzed by BZ-9000 fluorescent microscopy (KEYENCE). N-cadherin (d) and PS1 (c) immunoreactivities are co-localized at the cell-cell contact sites (arrowheads). Scale bar: 20  $\mu$ m.

distal subcellular compartments (Berezovska *et al.* 2003). In addition, we have shown that N-cadherin/PS1 interaction changes subcellular distribution of the PS1/ $\gamma$ -secretase, thereby enhancing its expression at the cell-surface (Uemura *et al.* 2007). Thus, we postulated that enhanced secretion of A $\beta$  in N-cadherin expressing cells may be attributed to better accessibility of APP to PS1/ $\gamma$ -secretase. To test this hypothesis we used an established FLIM assay to monitor APP-PS1

interactions (Berezovska *et al.* 2003). PS1 was immunostained with an anti-PS1 loop region antibody labeled with Alexa 488 (FRET donor) and the APP CT was immunostained with a Cy3-labeled antibody (FRET acceptor). The fluorescence lifetime of the Alexa488 donor fluorophore shortens in close vicinity (< 10 nm) of a FRET acceptor fluorophore. The degree of the lifetime shortening is a quantitative measure of proximity. The donor fluorophore

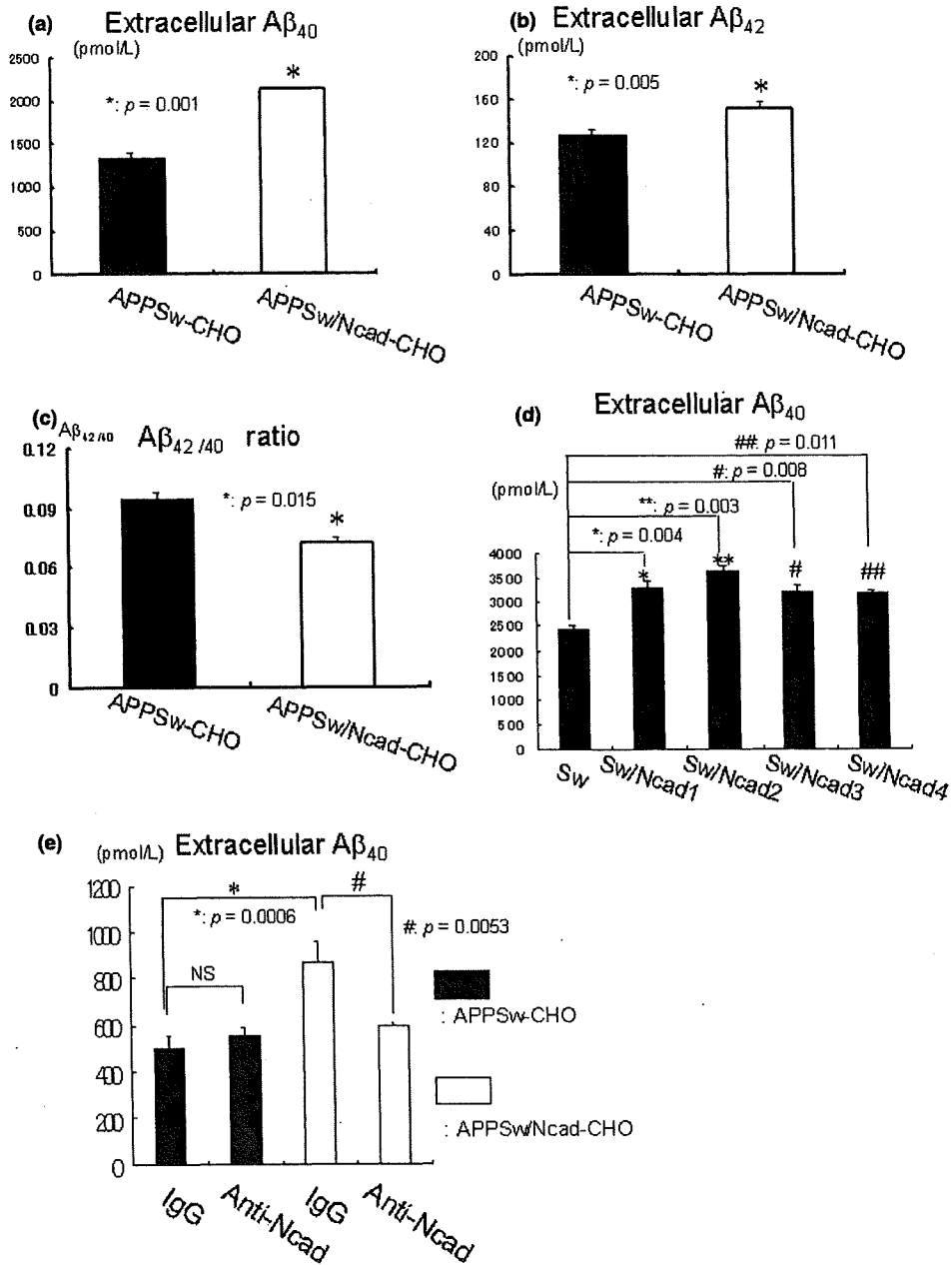


**Fig. 2** N-cadherin expression enhances extracellular Aβ levels and reduces Aβ<sub>42/40</sub> ratio. (a) APPSw-CHO cells or APPSw/Ncad-CHO cells were incubated in OPTI-MEM for 12 h. The amount of extracellular Aβ<sub>40</sub> was significantly elevated in APPSw/Ncad-CHO cells, compared with APPSw-CHO cells ( $n = 8$ ,  $*p = 0.001$ ). (b) APPSw-CHO cells or APPSw/Ncad-CHO cells were incubated in OPTI-MEM for 12 h. After incubation, culture medium was collected and the amount of extracellular Aβ<sub>42</sub> was measured. Extracellular Aβ<sub>42</sub> was significantly elevated in APPSw/Ncad-CHO cells, compared with APPSw-CHO cells ( $n = 8$ ,  $*p = 0.005$ ). (c) The Aβ<sub>42/40</sub> ratio in the medium was significantly decreased in APPSw/Ncad-CHO cells, compared with APPSw-CHO cells ( $n = 8$ ,  $*p = 0.015$ ). (d) APPSw-CHO (Sw) cells or four independent stable cell lines of APPSw/Ncad-

CHO cells (SwNcad1-4) were incubated in OPTI-MEM for 24 h. After incubation, the amount of extracellular Aβ<sub>40</sub> was measured. Secreted extracellular Aβ<sub>40</sub> was significantly elevated in every APPSw/Ncad-CHO stable cell line (SwNcad1-4), compared with that in APPSw-CHO cells (Sw) ( $n = 4$ ,  $*p = 0.004$ ,  $**p = 0.003$ ,  $#p = 0.003$ ,  $##p = 0.011$ ). (e) APPSw-CHO cells or APPSw/Ncad-CHO cells were incubated in fresh OPTI-MEM containing either control IgG or N-cadherin-neutralizing antibody for 6 h. After incubation, the amount of extracellular Aβ<sub>40</sub> was measured. N-cadherin-neutralizing antibody significantly reduced the extracellular Aβ<sub>40</sub> release into the medium in APPSw/Ncad-CHO cells ( $*p = 0.006$ ,  $n = 4$ ). Conversely, N-cadherin-neutralizing antibody had no effect on the extracellular Aβ<sub>40</sub> release into the medium in APPSw-CHO cells ( $#p = 0.0053$ ,  $n = 4$ ).

**Table 1** FRET between PS1 loop and APP CT in CHOSw compared with NcadCHOSw cells

Cell line	FRET donor (Alexa 488)	FRET acceptor (Cy3)	Alexa 488 lifetime in ps (mean $\pm$ SE)	p value (compared with CHOSw PS1 loop APP CT)
APPSw-CHO ( $n = 10$ )	PS1 loop	None (negative control)	1932 $\pm$ 7	$p < 0.0001$
APPSw-CHO ( $n = 10$ )	PS1 loop	APP CT	1790 $\pm$ 22	
APPSw/Ncad-CHO ( $n = 12$ )	PS1 loop	APP CT	1644 $\pm$ 25	$p < 0.0001$

lifetime can be color-coded and displayed on a pixel-by-pixel basis through the entire image of the cell: if APP and PS1 molecules are closer together, the donor fluorescence lifetime will be shorter, and the color will be closer to red. The FLIM analysis showed that Alexa 488 lifetime was significantly shortened in APPSw/Ncad-CHO cells, compared with that in APPSw-CHO cells, indicating that PS1 and APP came into closer proximity (or increased percentage of molecules are in close proximity to one another) in the presence of N-cadherin (Table 1). Pseudocolor FLIM image showed more red pixels per cell (i.e., more interacting molecules per cell) in APPSw/Ncad-CHO cells (Fig. 3b), compared with that in APPSw-CHO cells (Fig. 3a). This indicates that N-cadherin expression may increase the accessibility of PS1/ $\gamma$ -secretase to its substrate APP. In order to examine the effect of N-cadherin-mediated cell adhesion on APP/PS1 interaction, we also examined the proximity of APP and PS1 in the presence of N-cadherin-neutralizing antibody (GC-4). We performed two complementary FLIM experiments; one with immunohistochemistry using goat anti-PS-NT antibody and rabbit anti-APP-CT antibody (Table 2) and the other using live cells expressing APP-GFP and PS1-RFP (Table 3), in the presence of either GC-4 or normal mouse IgG as a control. In both blocking experiments, we observed significantly longer donor fluorophore lifetime in GC4 treated cells, comparing with that in IgG- treated cells, indicating that N-cadherin-based cell-cell adhesion specifically modulates the accessibility of APP to PS1/ $\gamma$ -secretase. To confirm these results biochemically, we transfected N-cadherin into HEK293 cells and analyzed whether N-cadherin expression enhances the APP-PS1 interaction by immunoprecipitation. As expected, APP-PS1 interaction was increased in N-cadherin expressing cells (Supporting information Fig. S2), indicating that N-cadherin expression brings APP and PS1/ $\gamma$ -secretase in closer proximity.

#### N-cadherin expression induces the conformational change of PS1

Whereas total A $\beta$  was increased in N-cadherin expressing cells, the A $\beta_{42/40}$  ratio was reduced (Fig. 2c). We and others have demonstrated previously that A $\beta_{42/40}$  ratio correlates with PS1 conformation in intact cells: familial Alzheimer's disease mutations in PS1 that elevate A $\beta_{42/40}$  ratio decreased (Berezovska *et al.* 2005), while A $\beta_{42}$ -lowering NSAIDs (Lleo *et al.* 2004) or structural changes

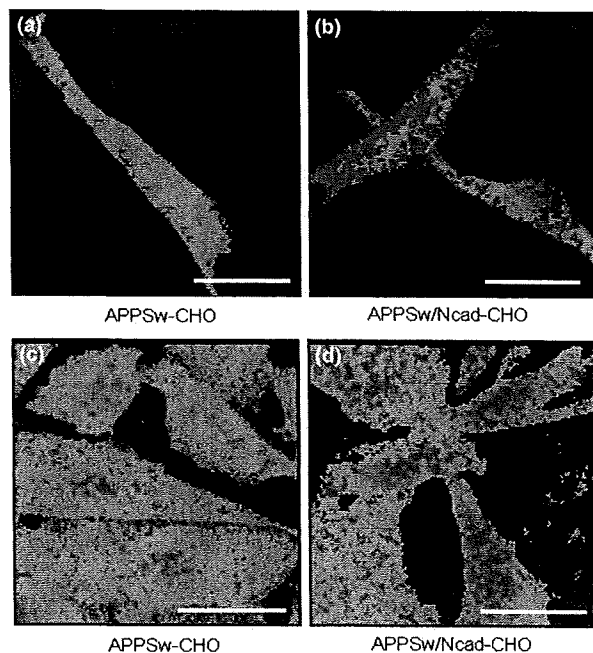


**Fig. 3** N-cadherin expression in CHO cells increases PS1-APP interactions and induces conformational change of PS1/ $\gamma$ -secretase. (a and b) For the FLIM assay, PS1 is stained at its loop region with Alexa 488 (FRET donor) and APP is stained at its CT with Cy3 (FRET acceptor). The fluorescence lifetime of Alexa 488 is displayed as a pseudocolor image: if PS1 and APP molecules are closer together, the donor fluorescence lifetime will be shorter, and the color will be closer to red. Alexa488 lifetime was significantly shortened in APPSw/Ncad-CHO cells (b), compared with that in APPSw-CHO cells (a), indicating that PS1 and APP came into closer proximity in the presence of N-cadherin. Scale bar: 10  $\mu$ m. (c and d) APPSw-CHO (c) or APPSw/Ncad-CHO (d) cells were immunostained with antibodies against PS1 NT (Alexa 488) and CT (Cy3). The proximity between PS1 NT and CT was evaluated by measuring lifetime of the Alexa 488 donor fluorophore (PS1 NT Alexa 488) in the FLIM assay. The fluorescence lifetime of Alexa 488 is displayed as a pseudocolor image. Red pixels indicate close proximity between PS1 N- and C-termini. Alexa 488 lifetime in APPSw/Ncad-CHO (d) cells was significantly increased, compared with that in APPSw-CHO cells (c), indicating that N-cadherin 'opened' PS1 conformation with NT and CT further apart. Scale bar: 10  $\mu$ m.

in  $\gamma$ -secretase component, Pen2 (Isoo *et al.* 2007) increased, PS1 NT-CT proximity. Therefore, we investigated whether change in A $\beta_{42/40}$  ratio observed in cells

**Table 2** FRET between PS1 N-terminus and APP CT in NcadCHOSw cells treated with N-cadherin neutralizing GC-4 antibody or IgG as a control

Cell line	FRET donor (Alexa 488)	FRET acceptor (Cy3)	Alexa 488 lifetime in ps (mean ± SE)	<i>p</i> value (compared with control IgG)
NcadCHOSw (Negative Control)	PS1 NT	None	1903 ± 28	<i>p</i> < 0.01
NcadCHOSw with control IgG ( <i>n</i> = 21)	PS1 NT	APP CT	1677 ± 22	
NcadCHOSw with GC-4 ( <i>n</i> = 17)	PS1 NT	APP CT	1789 ± 100	

**Table 3** FRET between PS1 loop and APP CT in living NcadCHOSw cells treated with GC-4 or IgG

Cell line	FRET donor	FRET acceptor	Alexa 488 lifetime in ps (mean ± SE)	<i>p</i> value (compared with control IgG)
NcadCHOSw (Negative Control)	APP-GFP	None	2076 ± 62	<i>p</i> < 0.01
NcadCHOSw with control IgG ( <i>n</i> = 21)	APP-GFP	PS1-RFP(loop)	1646 ± 223	
NcadCHOSw with GC-4 ( <i>n</i> = 17)	APP-GFP	PS1-RFP(loop)	1859 ± 74	

with tighter cell-cell adhesion mediated by N-cadherin is due to a conformational change in PS1/ $\gamma$ -secretase. The proximity between PS1 NT and CT in fixed and detergent permeabilized cells was evaluated by measuring lifetime of the Alexa 488 donor fluorophore (PS1 NT Alexa 488) in the absence (negative control) and presence of the Cy3 acceptor on the PS1 CT. As expected, the Alexa 488 donor fluorophore lifetime shortened when the PS1 CT was labeled with the Cy3 acceptor (Table 4), consistent with the close proximity between the PS1 NT and CT in APPSw-CHO cells. In contrast, Alexa 488 lifetime in APPSw/Ncad-CHO cells was significantly longer (1821 ± 14 ps), compared with that in APPSw-CHO cells, indicating that N-cadherin 'opened' the PS1 conformation with NT and CT being further apart (Tables 2 and 3, Fig. 3c and d). Thus, these results are in agreement with the previous findings that more 'open' PS1 conformation correlates with generation of the shorter A $\beta$  species (Lleo *et al.* 2004), and therefore decreased A $\beta_{42/40}$  ratio in APPSw/Ncad-CHO cells may be attributed to the change in conformation of the PS1/ $\gamma$ -secretase due to N-cadherin over-expression.

#### PS1/N-cadherin interaction affects both A $\beta$ production and A $\beta_{42/40}$ ratio

Since N-cadherin interacts with the cytoplasmic loop of PS1 CTF (Georgakopoulos *et al.* 1999), we next deter-

mined whether the PS1/N-cadherin interaction affects A $\beta$  production and/or A $\beta_{42/40}$  ratio. To test this, either wtPS1 or a PS1 mutant lacking the N-cadherin interaction domain [ $\Delta$ 340-350PS1, Uemura *et al.* 2007] was transfected into APPSw/Ncad-CHO cells. Since PS1/ $\gamma$ -secretase acts in a complex including PS1, Nicastrin, Pen-2 and Aph-1 (Takasugi *et al.* 2003),  $\Delta$ 340-350PS1 competes with endogenous wild-type PS1 to occupy other components of  $\gamma$ -secretase and act in a dominant-negative fashion (Thinakaran *et al.* 1997). As expected, immunoprecipitation assay revealed that  $\Delta$ 340-350PS1 does not interact with N-cadherin (Fig. 4a). We found that the extracellular levels of both A $\beta_{40}$  (Fig. 4b) and A $\beta_{42}$  (Fig. 4c) were decreased after the transient expression of  $\Delta$ 340-350PS1, compared with wtPS1. In addition, A $\beta_{42/40}$  ratio in the medium was increased in the  $\Delta$ 340-350PS1 transfectants, compared with that in wtPS1 (Fig. 4d), indicating that the PS1/N-cadherin interaction affects both A $\beta$  production and A $\beta_{42/40}$  ratio.

#### Discussion

In this report, we demonstrate that introducing N-cadherin into cadherin-deficient CHO cells increased secreted A $\beta_{40}$  and A $\beta_{42}$  levels (Fig. 2). The expression of N-cadherin in CHO cells elevates cell-surface levels of PS1/ $\gamma$ -secretase [Uemura *et al.* 2007], see also Fig. 1. Thus, the effect of

**Table 4** FRET between PS1 NT and CT in CHOSw compared with NcadCHOSw cells

Cell line	FRET donor (Alexa 488)	FRET acceptor (Cy3)	Alexa 488 lifetime in ps (mean ± SE)	<i>p</i> value (compared with NcadCHOSw)
APPSw-CHO ( <i>n</i> = 11)	PS1 NT	None (negative control)	1897 ± 7	<i>p</i> < 0.0001
APPSw-CHO ( <i>n</i> = 14)	PS1 NT	PS1 CT	1524 ± 46	
APPSw/Ncad-CHO ( <i>n</i> = 14)	PS1 NT	PS1 CT	1821 ± 14	

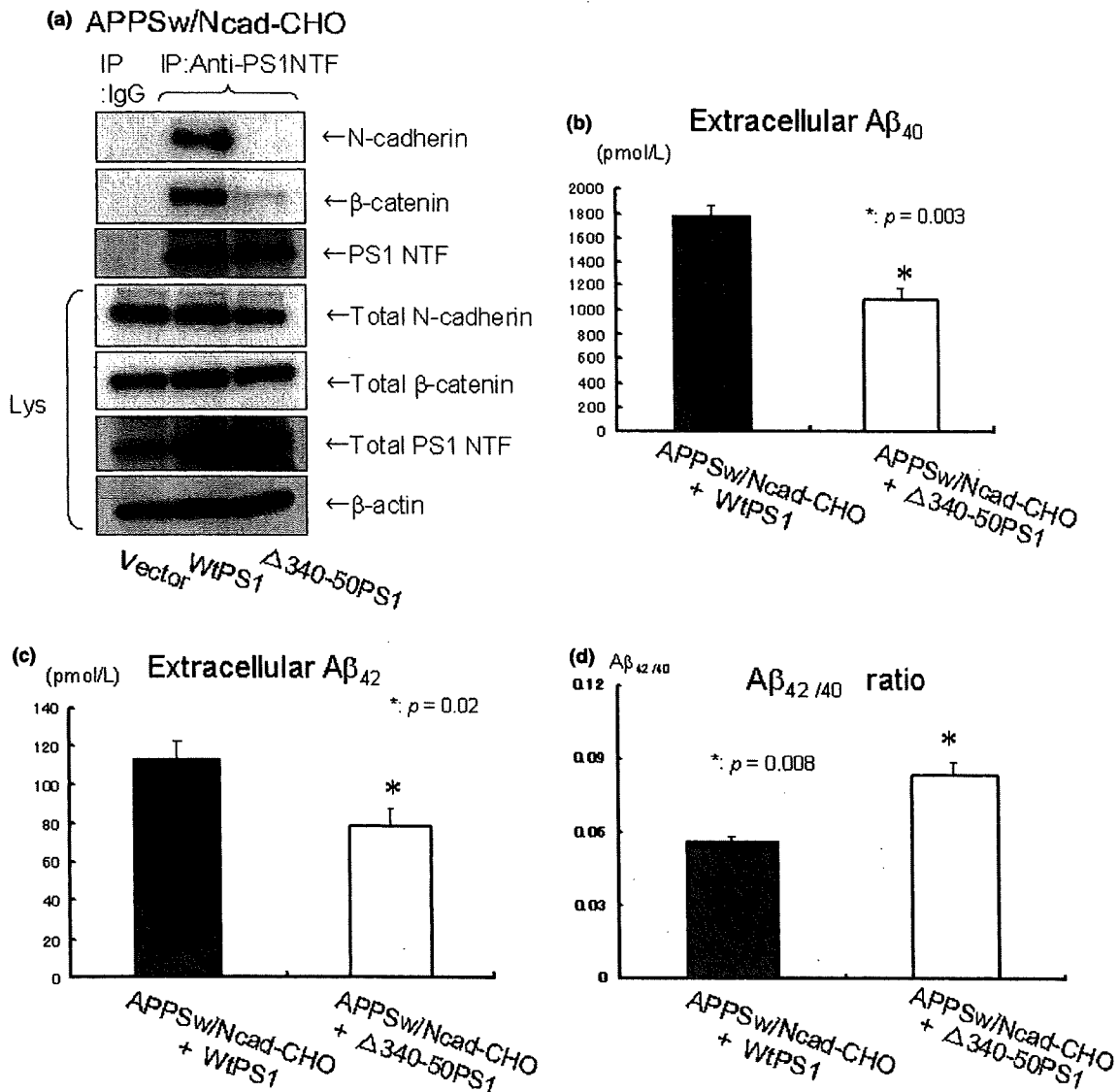


**Fig. 4** Loss of PS1/N-cadherin interaction reduces extracellular A $\beta$  levels and enhances A $\beta_{42/40}$  ratio. (a) APPSw/Ncad-CHO cells were transfected with either wtPS1 or PS1 mutant lacking PS1/N-cadherin interaction domain ( $\Delta$ 340-350PS1). 24 h after transfection, cell lysates were immunoprecipitated with rabbit polyclonal anti-PS1 NT antibody or normal rabbit IgG as a control, followed by the western blot. N-cadherin and  $\beta$ -catenin were efficiently co-immunoprecipitated with wild type PS1. However, very poor N-cadherin and  $\beta$ -catenin signal was detected in the co-immunoprecipitates from APPSw/Ncad-CHO cells transfected with  $\Delta$ 340-350PS1, indicating the lack of PS1/N-cadherin/ $\beta$ -catenin interaction. The expression levels of PS1, N-cadherin and  $\beta$ -catenin in the cell lysates (Lys) were similar between these cell lines. The bottom lane indicates the  $\beta$ -actin level, used as a loading control. (b)  $6 \times 10^5$  of APPSw/Ncad-CHO cells cultured in

the cadherin expression on A $\beta$  secretion might be mediated by the change in the subcellular distribution of PS1/ $\gamma$ -secretase. In addition, our FLIM analysis revealed

3.5 cm dish were transfected with either wtPS1 or PS1 mutant lacking PS1/N-cadherin interaction domain ( $\Delta$ 340-350PS1). 24 h after transfection, cells were washed once with OPTI-MEM and incubated in fresh OPTI-MEM for 12 h. After incubation, the culture medium was collected and the amount of extracellular A $\beta_{40}$  was measured by ELISA. Extracellular A $\beta_{40}$  was significantly reduced in the background of  $\Delta$ 340-350PS1 transfection, compared with that in wtPS1 transfected cells (\* $p = 0.003$ ,  $n = 4$ ). (c) The amount of extracellular A $\beta_{42}$  in the same condition as in (b) was measured by ELISA. Extracellular A $\beta_{42}$  was significantly reduced in the background of  $\Delta$ 340-350PS1 transfection, compared with that in wtPS1 transfected cells (\* $p = 0.02$ ,  $n = 4$ ). (d) The A $\beta_{42/40}$  ratio in the conditions (b) and (c) was significantly reduced in the background of  $\Delta$ 340-350PS1 transfection (\* $p = 0.008$ ,  $n = 4$ ).

that the N-cadherin expression allowed more PS1 and APP to interact near the cell surface, resulting in a greater amount of fluorophore-labeled epitopes coming into close



proximity (Table 1 and see more red pixels in Fig. 3b compared with 3a). The FLIM results were confirmed by co-IP experiment (Supporting information Fig. S2), indicating better accessibility of APP to PS1/ $\gamma$ -secretase in the presence of N-cadherin. These data suggest that subcellular redistribution and better accessibility of PS1/ $\gamma$ -secretase to APP substrate may be the cause of the net increase in total A $\beta$  production in the presence of N-cadherin. The cellular compartment in which APP/PS1 interactions are promoted by N-cadherin was not clarified in the present study. However, since N-cadherin is an important cell adhesion molecule and we have previously demonstrated that N-cadherin promotes cell-surface expression of PS1/ $\gamma$ -secretase ((Uemura *et al.* 2007), see also Fig. 1), the interactions are likely to occur near to the cell surface.

Interestingly, N-cadherin expression not only enhanced A $\beta$  release, but also decreased A $\beta_{42/40}$  ratio, the latter effect is similar to NSAIDs treatment (Lleo *et al.* 2004) and opposite to that caused by the FAD-linked PS1 mutations (Berezovska *et al.* 2005). This effect was associated with the 'open' PS1 conformation, driving NT and CT further apart, in N-cadherin expressing cells as revealed by the FLIM assay (Tables 2 and 3 and Fig. 3c and d). Preventing N-cadherin-PS1 interaction either by absence of N-cadherin (Fig. 1) or by introducing a PS1 mutant that does not interact with N-cadherin (Fig. 4) both have increased A $\beta_{42/40}$  ratio. In the absence of N-cadherin (APPSw-CHO cells), the A $\beta_{42/40}$  ratio was around  $0.095 \pm 0.006$ , whereas it was reduced to  $0.072 \pm 0.006$  in the presence of N-cadherin (APPSw/Ncad-CHO cells) (Fig. 2c). The A $\beta_{42/40}$  ratio under the expression of  $\Delta 340-350$ PS1 was  $0.083 \pm 0.009$ , whereas A $\beta_{42/40}$  ratio under the expression of wt PS1 was  $0.056 \pm 0.004$  (Fig. 4d). These results indicate that  $\Delta 340-350$  mutant prevented the decrease in A $\beta_{42/40}$  ratio induced by N-cadherin expression and restored to baseline A $\beta_{42/40}$  ratio. Since N-cadherin binds to the cytoplasmic loop of PS1 CT (Georgakopoulos *et al.* 1999), it is possible that this physical contact causes an allosterical change in PS1 conformation by moving PS1 NT and CT further apart. On the contrary to the N-cadherin expression, the expression of wt PS1 has no effect on A $\beta$  production. Other reports have also demonstrated that single expression of wt PS1 has limited effect on A $\beta$  production *in vivo* (Citron *et al.* 1997). We speculate that this apparent contradiction is caused by the lack of other  $\gamma$ -secretase components, when PS1 is expressed alone.  $\gamma$ -secretase is composed of PS1, nicastrin, pen-2 and aph-1 and can remain stable only when these components are available. It was also reported that expression of pen-2 is required for conferring the  $\gamma$ -secretase activity and endoproteolysis of PS1 (Takasugi *et al.* 2003). Thus, expression of PS1 alone might not have impact on A $\beta$  metabolism significantly.

Thus, expression of N-cadherin modulates A $\beta$  production in two ways: the total amount of A $\beta$  and the A $\beta_{42/40}$  ratio. These are independent readouts of  $\gamma$ -secretase function. According to our experimental data, these changes can be interpreted as reflecting access of N-terminally cleaved APP to functionally active  $\gamma$ -secretase (total amount of A $\beta$ ) compared with the exact molecular interaction between PS-1 and the APP substrate (A $\beta_{42/40}$  ratio). The presence of N-cadherin impacts each of these features, by directing the localization of  $\gamma$ -secretase closer to cell surface membrane as well as a direct allosteric effect on PS-1/ $\gamma$ -secretase conformation. Accumulating evidence suggests that partial loss of function in PS1/ $\gamma$ -secretase may lead to increased A $\beta_{42/40}$  ratio as well as to neurodegeneration (Shen and Kelleher 2007; Wolfe 2007). In addition, a recent report suggests that A $\beta_{40}$  may inhibit amyloid deposition and thus may be physiologically neuroprotective (Kim *et al.* 2007). In this respect, tight cell-cell contact may enhance the function of PS1/ $\gamma$ -secretase to produce more A $\beta_{40}$  by inducing its distributional and conformational change.

It has recently been shown that neuronal activity modulates the production and secretion of A $\beta$  peptides (Kamenetz *et al.* 2003; Lesne *et al.* 2005). In addition, it was demonstrated *in vivo* that A $\beta$  levels in the brain interstitial fluid are dynamically influenced by synaptic activity (Cirrito *et al.* 2005). Taken together, A $\beta$  secretion seems to be physiologically regulated in neurons and A $\beta$  itself may have its own physiological function (Pearson and Peers 2006). On the contrary, converging lines of evidence suggests that natural soluble A $\beta$  oligomers trigger synaptic loss (Spires *et al.* 2005; Shankar *et al.* 2007). Therefore, it is plausible that synaptic dissociation caused by A $\beta$  oligomers changes PS1 conformation to produce more A $\beta_{42}$ , thus starting the vicious cycle of A $\beta_{42}$  generation by modifying the A $\beta_{42/40}$  ratio. Our present study presents solid evidence that A $\beta$  production and the A $\beta_{42/40}$  ratio can be modulated by the degree of PS1-N-cadherin interaction, and thus potentially by cell-cell adhesion status. Our current findings, thus, provide a potential link between synaptic contacts and physiological A $\beta$  release, with cadherins being the key player. However, these experiments are carried out by CHO cell lines exogenously expressed with APP or its mutant, which does not allow to conclude about the relevance of the presented mechanism in neurons and remain to be proved in neuron and *in vivo* settings.

With its potential role in the rearrangement of existing cell-cell contacts (Okamoto *et al.* 2001; Marambaud *et al.* 2002; Haas *et al.* 2005) PS1/ $\gamma$ -secretase may influence synaptic plasticity, which might be affected in AD. Future study in this field could lead to a better understanding of AD synaptic pathophysiology.

## Acknowledgments

Research described in this article was supported by Philip Morris USA Inc., Philip Morris International (OB, SS) and NIH AG026593 (OB) and by the Ministry of Education, Science, Sports and Culture (Japan), Grant-in-Aid for 18023021, 18059019 (AK). We thank Dr Kaether (Ludwig-Maximilians University, Germany) for generously providing original PS1-GFP construct.

## Supporting information

Additional Supporting information may be found in the online version of this article:

**Fig. S1** N-cadherin expression reduces A $\beta_{42/40}$  ratio in the background of wild-type APP expression.

**Fig. S2** N-cadherin expression increases APP-PS1 interaction.

Please note: Wiley-Blackwell are not responsible for the content or functionality of any supplementary materials supplied by the authors. Any queries (other than missing material) should be directed to the corresponding author for the article.

## References

- Berezovska O., Ramdya P., Skoch J., Wolfe M. S., Bacskai B. J. and Hyman B. T. (2003) Amyloid precursor protein associates with a nicastrin-dependent docking site on the presenilin 1-gamma-secretase complex in cells demonstrated by fluorescence lifetime imaging. *J. Neurosci.* **23**, 4560–4566.
- Berezovska O., Lleo A., Herl L. D., Frosch M. P., Stern E. A., Bacskai B. J. and Hyman B. T. (2005) Familial Alzheimer's disease presenilin 1 mutations cause alterations in the conformation of presenilin and interactions with amyloid precursor protein. *J. Neurosci.* **25**, 3009–3017.
- Bozdagi O., Shan W., Tanaka H., Benson D. L. and Huntley G. W. (2000) Increasing numbers of synaptic puncta during late-phase LTP: N-cadherin is synthesized, recruited to synaptic sites, and required for potentiation. *Neuron* **28**, 245–259.
- Cirrito J. R., Yamada K. A., Finn M. B., Sloviter R. S., Bales K. R., May P. C., Schoepp D. D., Paul S. M., Mennerick S. and Holtzman D. M. (2005) Synaptic activity regulates interstitial fluid amyloid-beta levels in vivo. *Neuron* **48**, 913–922.
- Citron M., Westaway D., Xia W. *et al.* (1997) Mutant presenilins of Alzheimer's disease increase production of 42-residue amyloid beta-protein in both transfected cells and transgenic mice. *Nat. Med.* **3**, 67–72.
- De Strooper B., Saftig P., Craessaerts K., Vanderstichele H., Guhde G., Annaert W., Von Figura K. and Van Leuven F. (1998) Deficiency of presenilin-1 inhibits the normal cleavage of amyloid precursor protein. *Nature* **391**, 387–390.
- De Wever O., Westbroek W., Verloes A., Bloemen N., Bracke M., Gespach C., Bruyneel E. and Mareel M. (2004) Critical role of N-cadherin in myofibroblast invasion and migration in vitro stimulated by colon-cancer-cell-derived TGF-beta or wounding. *J. Cell Sci.* **117**, 4691–4703.
- Georgakopoulos A., Marambaud P., Efthimiopoulos S. *et al.* (1999) Presenilin-1 forms complexes with the cadherin/catenin cell-cell adhesion system and is recruited to intercellular and synaptic contacts. *Mol Cell* **4**, 893–902.
- Haas I. G., Frank M., Veron N. and Kemler R. (2005) Presenilin-dependent processing and nuclear function of gamma-protocadherins. *J. Biol. Chem.* **280**, 9313–9319.
- Isoo N., Sato C., Miyashita H., Shinohara M., Takasugi N., Morohashi Y., Tsuji S., Tomita T. and Iwatsubo T. (2007) Abeta42 overproduction associated with structural changes in the catalytic pore of gamma-secretase: common effects of Pen-2 N-terminal elongation and fenofibrate. *J. Biol. Chem.* **282**, 12388–12396.
- Kamenetz F., Tomita T., Hsieh H., Seabrook G., Borchelt D., Iwatsubo T., Sisodia S. and Malinow R. (2003) APP processing and synaptic function. *Neuron* **37**, 925–937.
- Kim J., Onstead L., Randle S., Price R., Smithson L., Zwizinski C., Dickson D. W., Golde T. and McGowan E. (2007) Abeta40 inhibits amyloid deposition in vivo. *J. Neurosci.* **27**, 627–633.
- Kinoshita A., Whelan C. M., Smith C. J., Berezovska O. and Hyman B. T. (2002) Direct visualization of the gamma secretase-generated carboxyl-terminal domain of the amyloid precursor protein: association with Fe65 and translocation to the nucleus. *J. Neurochem.* **82**, 839–847.
- Lesne S., Ali C., Gabriel C., Croci N., MacKenzie E. T., Glabe C. G., Plotkine M., Marchand-Verrecchia C., Vivien D. and Buisson A. (2005) NMDA receptor activation inhibits alpha-secretase and promotes neuronal amyloid-beta production. *J. Neurosci.* **25**, 9367–9377.
- Lleo A., Berezovska O., Herl L., Raju S., Deng A., Bacskai B. J., Frosch M. P., Irizarry M. and Hyman B. T. (2004) Nonsteroidal anti-inflammatory drugs lower Abeta42 and change presenilin 1 conformation. *Nat. Med.* **10**, 1065–1066.
- Marambaud P., Shioi J., Serban G. *et al.* (2002) A presenilin-1/gamma-secretase cleavage releases the E-cadherin intracellular domain and regulates disassembly of adherens junctions. *EMBO J.* **21**, 1948–1956.
- Okamoto I., Kawano Y., Murakami D., Sasayama T., Araki N., Miki T., Wong A. J. and Saya H. (2001) Proteolytic release of CD44 intracellular domain and its role in the CD44 signaling pathway. *J. Cell Biol.* **155**, 755–762.
- Pearson H. A. and Peers C. (2006) Physiological roles for amyloid beta peptides. *J. Physiol.* **575**, 5–10.
- Shankar G. M., Bloodgood B. L., Townsend M., Walsh D. M., Selkoe D. J. and Sabatini B. L. (2007) Natural oligomers of the Alzheimer amyloid-beta protein induce reversible synapse loss by modulating an NMDA-type glutamate receptor-dependent signaling pathway. *J. Neurosci.* **27**, 2866–2875.
- Shen J. and Kelleher R. J. (2007) The presenilin hypothesis of Alzheimer's disease: evidence for a loss-of-function pathogenic mechanism. *Proc. Natl Acad. Sci. USA* **104**, 403–409.
- Spires T. L., Meyer-Luehmann M., Stern E. A., McLean P. J., Skoch J., Nguyen P. T., Bacskai B. J. and Hyman B. T. (2005) Dendritic spine abnormalities in amyloid precursor protein transgenic mice demonstrated by gene transfer and intravital multiphoton microscopy. *J. Neurosci.* **25**, 7278–7287.
- Takasugi N., Tomita T., Hayashi I., Tsuruoka M., Niimura M., Takahashi Y., Thinakaran G. and Iwatsubo T. (2003) The role of presenilin cofactors in the gamma-secretase complex. *Nature* **422**, 438–441.
- Thinakaran G., Borchelt D. R., Lee M. K. *et al.* (1996) Endoproteolysis of presenilin 1 and accumulation of processed derivatives in vivo. *Neuron* **17**, 181–190.
- Thinakaran G., Harris C. L., Ratovitski T., Davenport F., Slunt H. H., Price D. L., Borchelt D. R. and Sisodia S. S. (1997) Evidence that levels of presenilins (PS1 and PS2) are coordinately regulated by competition for limiting cellular factors. *J. Biol. Chem.* **272**, 28415–28422.
- Togashi H., Abe K., Mizoguchi A., Takaoka K., Chisaka O. and Takeichi M. (2002) Cadherin regulates dendritic spine morphogenesis. *Neuron* **35**, 77–89.
- Uemura K., Kitagawa N., Kohno R., Kuzuya A., Kageyama T., Chonabayashi K., Shibasaki H. and Shimohama S. (2003) Presenilin 1 is involved in maturation and trafficking of N-cadherin to the plasma membrane. *J. Neurosci. Res.* **74**, 184–191.

- Uemura K., Kihara T., Kuzuya A., Okawa K., Nishimoto T., Bito H., Ninomiya H., Sugimoto H., Kinoshita A. and Shimohama S. (2006a) Activity-dependent regulation of beta-catenin via epsilon-cleavage of N-cadherin. *Biochem. Biophys. Res. Commun.* **345**, 951–958.
- Uemura K., Kihara T., Kuzuya A., Okawa K., Nishimoto T., Ninomiya H., Sugimoto H., Kinoshita A. and Shimohama S. (2006b) Characterization of sequential N-cadherin cleavage by ADAM10 and PS1. *Neurosci. Lett.* **402**, 278–283.
- Uemura K., Kuzuya A., Shimozone Y., Aoyagi N., Ando K., Shimohama S. and Kinoshita A. (2007) GSK3beta Activity Modifies the Localization and Function of Presenilin 1. *J. Biol. Chem.* **282**, 15823–15832.
- Wolfe M. S. (2007) When loss is gain: reduced presenilin proteolytic function leads to increased Abeta42/Abeta40. Talking Point on the role of presenilin mutations in Alzheimer disease. *EMBO Rep* **8**, 136–140.



Contents lists available at ScienceDirect

## Autonomic Neuroscience: Basic and Clinical

journal homepage: [www.elsevier.com/locate/autneu](http://www.elsevier.com/locate/autneu)

## Autoimmune autonomic ganglionopathy with Sjögren's syndrome: Significance of ganglionic acetylcholine receptor antibody and therapeutic approach

Takayuki Kondo <sup>a</sup>, Haruhisa Inoue <sup>a,\*</sup>, Takashi Usui <sup>b</sup>, Tsuneyo Mimori <sup>b</sup>, Hidekazu Tomimoto <sup>a</sup>, Steven Vernino <sup>c</sup>, Ryosuke Takahashi <sup>a</sup>

<sup>a</sup> Department of Neurology, Kyoto University Hospital, Kyoto, Japan

<sup>b</sup> Department of Rheumatology and Clinical Immunology, Kyoto University Hospital, Kyoto, Japan

<sup>c</sup> University of Texas Southwestern Medical Center, Dallas, TX, USA

## ARTICLE INFO

## Article history:

Received 4 August 2008

Received in revised form 29 November 2008

Accepted 1 December 2008

## Keywords:

Ganglionic acetylcholine receptor antibody

Autoimmune autonomic ganglionopathy

Sjögren's syndrome

Prednisolone

## ABSTRACT

Autoimmune autonomic ganglionopathy (AAG) is a disorder defined by antibodies to the nicotinic acetylcholine receptor of the autonomic ganglia. We report two patients with chronically progressing dysautonomia with Sjögren's syndrome (SS). The first case showed elevated titer of ganglionic acetylcholine receptor (AChR) antibody and improved with oral intake of prednisolone. In contrast, the second case showed no elevation of ganglionic AChR antibody titer and had poor response to immunomodulatory therapy. These two cases indicate that chronic AAG may be treatable by immunomodulatory therapy, and have relevance to SS.

© 2008 Elsevier B.V. All rights reserved.

### 1. Introduction

Peripheral autonomic failures have various backgrounds such as diabetes mellitus, amyloidosis, inherited autonomic neuropathy or autoimmune disorders (e.g. Guillain-Barré syndrome, paraneoplastic syndrome, Sjögren's syndrome etc.). In this decade Vernino et al. proposed a novel disease entity of autoimmune autonomic failure, characterized by positive ganglionic acetylcholine receptor (AChR) antibody in the serum (Vernino et al., 2000) and designated autoimmune autonomic ganglionopathy (AAG). Ganglionic AChR antibody binds to alpha 3 subunits of the nicotinic acetylcholine receptor, which is localized to the postsynaptic neuron in the autonomic nerve ganglion, and disturbs the function of postganglionic autonomic nerves. Serum levels of the ganglionic AChR antibody significantly correlates with both neurological severity and clinical course (high titer; severe symptoms with acute or subacute progression, low titer; mild symptoms with chronic progression) (Low et al., 2003).

Here we present two Japanese patients with Sjögren's syndrome (SS), who also developed gradually progressive autonomic dysfunction. Detailed evaluation revealed clear differences between these two similar cases; one showed elevated titer of ganglionic AChR antibody, improved by oral prednisolone, whereas the other did not show elevation of ganglionic AChR antibody titer and had poor response to

immunomodulatory therapy. In the analysis of these two patients, we discussed the potential relationships between ganglionic AChR and SS.

### 2. Case presentation

#### 2.1. Patient 1

A 74-year-old healthy man has suffered from oral sicca symptom and chronically progressive orthostatic dizziness for 3 years. When changing from the supine to the standing position, he lost consciousness and his blood pressure became too low to be measured. Physiological evaluation revealed orthostatic hypotension (supine position; blood pressure 90/60 mmHg and heart rate 61/min, standing position; 40/30 mmHg and 63/min), tonic pupil (3/3 mm), dry mouth, dry skin, urinary frequency (more than 6 times a night) and constipation. There were no other abnormal findings on neurologic examination. Routine laboratory examinations of blood, CSF and urine showed no abnormal findings. Anti muscarinic acetylcholine receptor M3 antibody was not examined. Plasma noradrenaline concentration decreased to 116 pg/ml (normal 140–570) at rest and failed to respond to tilting. There was no conspicuous abnormality in brain magnetic resonance imaging (MRI), single photon emission computed tomography (IMP-SPECT; imaging for cerebral blood flow) and peripheral nerve conduction studies. Cardiac uptake of 123I-metaiodobenzylguanidine (MIBG) scintigraphy decreased, with heart to mediastinum (H/M) ratio at 1.73 (examined at 15 min after injection, normal H/M > 1.92). The R-R interval variation on the electrocardiogram was 0.62% at rest. Tonic pupil responded to

\* Corresponding author. Tel.: +81 75 751 3768.

E-mail address: [haruhisa@kuhp.kyoto-u.ac.jp](mailto:haruhisa@kuhp.kyoto-u.ac.jp) (H. Inoue).